

Beating the 3 dB Limit for Intracavity Squeezing and Its Application to Nondemolition Qubit Readout

Wei Qin,¹ Adam Miranowicz,^{1,2} and Franco Nori^{1,3}

¹*Theoretical Quantum Physics Laboratory, RIKEN Cluster for Pioneering Research, Wako-shi, Saitama 351-0198, Japan*

²*Faculty of Physics, Adam Mickiewicz University, 61-614 Poznań, Poland*

³*Department of Physics, The University of Michigan, Ann Arbor, Michigan 48109-1040, USA*

(Dated: March 15, 2022)

While the squeezing of a propagating field can, in principle, be made arbitrarily strong, the cavity-field squeezing is subject to the well-known 3 dB limit, and thus has limited applications. Here, we present a novel method to beat this limit using a fully quantum degenerate parametric amplifier (DPA). Specifically, we show that by *simply* applying a two-tone driving to the signal mode, the pump mode can, *counterintuitively*, be driven by the photon loss of the signal mode into a steady squeezed state with, in principle, an *arbitrarily high* degree of squeezing. Furthermore, we demonstrate that this intracavity squeezing can increase the signal-to-noise ratio of longitudinal qubit readout *exponentially* with the degree of squeezing. Correspondingly, an improvement of the measurement error by *many orders of magnitude* can be achieved even for modest parameters. In stark contrast, using intracavity squeezing of the semiclassical DPA *cannot* practically increase the signal-to-noise ratio and thus improve the measurement error. Our results extend the range of applications of DPAs and open up new opportunities for modern quantum technologies.

Introduction.—Squeezed states of light [1] form a fundamental building block in modern quantum technologies ranging from quantum metrology [2, 3] to quantum information processing [4, 5]. In particular, squeezing of a propagating field can in principle be made arbitrarily strong, and therefore has been widely used for, e.g., gravitational-wave detection [6–8], mechanical cooling [9, 10], nondemolition qubit readout [11–14], and even demonstrating quantum supremacy via Gaussian boson sampling [15, 16]. However, these applications inherently suffer from transmission and injection losses, because externally generated squeezed light needs to be transmitted and then injected into the systems under consideration. Such losses are a major obstacle to using extremely fragile squeezed states. To address this problem, exploiting intracavity squeezing (i.e., squeezing of a cavity field) offers a promising route.

To date, intracavity squeezing of light has been applied, e.g., to cool mechanical resonators [17–19], enhance light-matter interactions [20–27], improve high-precision measurements [28–30], and generate non-classical states [31–34]. Despite such considerable developments, the range and quality of applications of intracavity squeezing are still largely limited by the steady-state squeezing of at most 3 dB (i.e., one half of the zero-point fluctuations) [35–37]. However, beating this 3 dB limit remains challenging, because the cavity photon loss, which is always present, destroys the essence of squeezing, i.e., two-photon correlations. In this manuscript, we show that, if such a photon loss is exploited as a resource rather than as a noise source, a strong steady-state intracavity squeezing exceeding 3 dB can be achieved.

In our approach, we consider a fully quantum DPA, where both pump and signal modes are quantized. We

demonstrate that a strong photon loss of the signal mode can steer the pump mode into a steady squeezed state, with a noise level reduced far beyond the 3 dB limit. In this way, an *arbitrarily strong* steady-state squeezing of the pump mode can in principle be achieved. To beat the 3 dB limit of intracavity squeezing, a theoretical approach, that requires a fast modulation of the coupling between the cavity and its environment, has been proposed [38]; and very recently, an experimental demonstration with three microwave modes coupled via a Josephson ring modulator was reported in Ref. [39]. As opposed to these previous studies, our approach relies only on common degenerate parametric amplification processes. More remarkably, we show that only a two-tone driving, if applied to the signal mode, can result in a strong steady-state squeezing for the pump mode. This is rather *counterintuitive*; indeed, common sense suggests that, as mentioned above, the steady-state intracavity squeezing of a DPA is usually limited to 3 dB.

Fast and high-fidelity nondemolition qubit readout is an essential prerequisite for quantum error correction [40, 41] and fault-tolerant quantum computation [42, 43]. Using squeezed light to improve such a readout is a long-standing goal [11–13, 44]. However, the simplest strategy, known as dispersive qubit readout [44, 45], gives rise to a qubit-state-dependent rotation of squeezing, such that the amplified noise in the antisqueezed quadrature is introduced into the signal quadrature, ultimately limiting the improvement of the signal-to-noise ratio (SNR). Thus, related experimental demonstrations in this context have remained elusive. Until recently, an improvement, enabled by injecting squeezed light into a cavity, was realized [46] for longitudinal qubit readout [13, 44, 47–49], which is drastically different from the dispersive readout and can enable much shorter

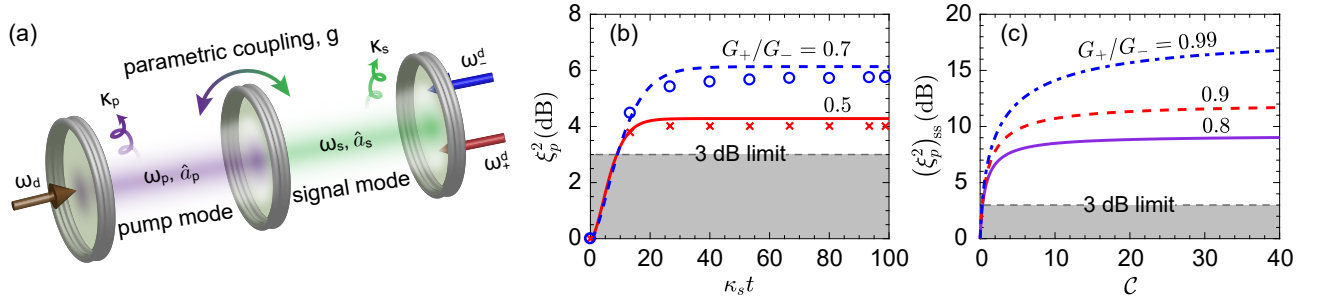


FIG. 1. (a) Schematic of our proposal with a fully quantum DPA. For clarity, we use two cavities representing the pump mode \hat{a}_p (frequency ω_p , loss rate κ_p) and the signal mode \hat{a}_s (frequency ω_s , loss rate κ_s), respectively. The single-photon parametric coupling between them has a strength g . A driving tone at frequency ω_d is applied to the pump mode and, simultaneously, the signal mode is driven by the other two tones at frequencies ω_{\pm}^d . (b) Time evolution of the squeezing parameter ξ_p^2 for $G_+/G_- = 0.5$ and 0.7 . We assumed that $\Delta_s = 100g$, $\Delta_p = 0.1\Delta_s$, $\Omega_{2pd} = 0.05\Delta_s$, $\kappa_s = 100\kappa_p = 0.4g$, and $G_- = g_0$. Solid and dashed curves are effective predictions, while symbols are the exact results. (c) Steady-state squeezing parameter $(\xi_p^2)_{ss}$ as a function of the cooperativity \mathcal{C} for $\kappa_s = 100\kappa_p$, and for $G_+/G_- = 0.8, 0.9$, and 0.99 . In (b) and (c), the gray shaded areas refer to the regime below the 3 dB limit; clearly, intracavity squeezing can exceed 3 dB.

measurement times. However, due to the presence of transmission and injection losses, more than half of the amount of squeezing is inefficient, and as a result the reported SNR is increased only by $\simeq 25\%$.

Here, we propose to apply the strong intracavity squeezing generated by our method to longitudinal qubit readout, thus avoiding the transmission and injection losses. We demonstrate that the SNR can be increased *exponentially* with the degree of intracavity squeezing. As a direct result, the measurement error is improved by *many orders of magnitude* for modest parameters. In sharp contrast, intracavity squeezing of the semiclassical DPA *cannot* significantly improve the SNR during a practically feasible measurement time, even though squeezing of the output field is very strong. Our main results are summarized in Table I in [50].

Physical model.—A fully quantum DPA, as shown in Fig. 1(a), consists of a pump mode \hat{a}_p and a signal mode \hat{a}_s , which are coupled through a single-photon parametric coupling of strength g . We assume that the pump mode is driven by a tone of frequency ω_d and amplitude \mathcal{E}_d , and at the same time the signal mode is subject to a two-tone driving of frequencies ω_{\pm}^d and amplitudes \mathcal{E}_{\pm} . The corresponding Hamiltonian in a frame rotating at ω_d is $\hat{H} = \hat{H}_0 + \hat{H}_{2td}$, with

$$\hat{H}_0 = \Delta_p \hat{a}_p^\dagger \hat{a}_p + \Delta_s \hat{a}_s^\dagger \hat{a}_s + g (\hat{a}_s^2 \hat{a}_p^\dagger + \text{H.c.}) + (\mathcal{E}_d \hat{a}_p^\dagger + \text{H.c.}), \quad (1)$$

$$\hat{H}_{2td} = \Omega_{2td}(t) \hat{a}_s^\dagger + \text{H.c.}, \quad (2)$$

where $\Delta_p = \omega_p - \omega_d$, $\Delta_s = \omega_s - \omega_d/2$, $\Omega_{2td}(t) = \mathcal{E}_- \exp(-i\omega_- t) + \mathcal{E}_+ \exp(-i\omega_+ t)$. Here, ω_p, ω_s are the resonance frequencies of the pump and signal modes, and $\omega_{\pm} = \omega_{\pm}^d - \omega_d/2$. We describe the photon losses of these two modes with the Lindblad dissipator $\mathcal{L}(\hat{o})\hat{\rho} = \hat{o}\hat{\rho}\hat{o}^\dagger - \frac{1}{2}(\hat{o}^\dagger\hat{o}\hat{\rho} + \hat{\rho}\hat{o}^\dagger\hat{o})$, so that the dynamics of the system can be determined by the master equation

$\dot{\hat{\rho}} = -i[\hat{H}, \hat{\rho}] + \kappa_p \mathcal{L}(\hat{a}_p)\hat{\rho} + \kappa_s \mathcal{L}(\hat{a}_s)\hat{\rho}$, where κ_p and κ_s are the photon-loss rates. Upon introducing the displacement transformation $\hat{a}_p \rightarrow \hat{a}_p + \alpha_p^d$, where $\alpha_p^d = \mathcal{E}_d / (i\kappa_p/2 - \Delta_p)$, the Hamiltonian \hat{H}_0 is transformed to $\hat{H}_0 = \Delta_p \hat{a}_p^\dagger \hat{a}_p + \hat{H}_{2pd} + \hat{V}$. Here,

$$\hat{H}_{2pd} = \Delta_s \hat{a}_s^\dagger \hat{a}_s + \Omega_{2pd} (\hat{a}_s^2 + \text{H.c.}), \quad (3)$$

$$\hat{V} = g (\hat{a}_s^2 \hat{a}_p^\dagger + \text{H.c.}), \quad (4)$$

where $\Omega_{2pd} = g\alpha_p^d$ is the strength of the many-photon parametric coupling that can be thought of as a two-photon driving of the signal mode \hat{a}_s . We have assumed, for simplicity, that α_p^d is real.

Since the single-photon coupling g is usually weak, the most studied regime of the DPA is for $\alpha_p^d \gg 1$. It is then standard to drop \hat{V} , leaving only \hat{H}_{2pd} . In this case, the pump mode is treated as a classical field, and the DPA is referred to as semiclassical. For such a semiclassical DPA, quantum noise of the intracavity signal field cannot be reduced below one half of the zero-point fluctuations in the steady state, corresponding to the 3 dB limit (see Refs. [36, 50]). The essential reason for this moderate squeezing is the photon loss of the signal mode; that is, the leakage of some single photons of correlated photon pairs out of the cavity causes a partial loss of two-photon correlations, thus lowering the degree of squeezing. In stark contrast, as we demonstrate below, this photon loss of the signal mode, when turned from a noise source into a resource, can lead to a steady-state squeezing of a quantized pump mode, which well exceeds 3 dB.

Squeezing far beyond 3 dB.—Recently, it has been shown experimentally that the available single-photon coupling g can range from tens of kHz to tens of MHz [51–58]. These advances allow one to consider the effect of the coupling \hat{V} in Eq. (4), e.g., for $\Delta_s = 0$ a strong two-photon loss [51–53, 59–62]. We here focus on the case

of $\Delta_s \neq 0$, and thus can introduce a signal Bogoliubov mode, $\hat{\beta}_s = \hat{a}_s \cosh(r_s) + \hat{a}_s^\dagger \sinh(r_s)$, with $\tanh(2r_s) = 2\Omega_{2\text{pd}}/\Delta_s$. The Hamiltonian $\hat{H}_{2\text{pd}}$ is then diagonalized, yielding $\hat{H}_{2\text{pd}} = \Lambda_s \hat{\beta}_s^\dagger \hat{\beta}_s$, where $\Lambda_s = \sqrt{\Delta_s^2 - 4\Omega_{2\text{pd}}^2}$. Below we restrict our discussion to the limit $\Omega_{2\text{pd}} \ll \Delta_s$, i.e., $r_s \ll 1$, such that the two-photon driving $\Omega_{2\text{pd}}$ results in a weak squeezing of the mode \hat{a}_s .

In this limit, the two-tone driving Hamiltonian $\hat{H}_{2\text{td}}$ and the coupling \hat{V} can be approximated by

$$\hat{H}_{2\text{td}} \simeq \cosh(r_s) \Omega_{2\text{td}}(t) \hat{\beta}_s^\dagger + \text{H.c.}, \quad (5)$$

$$\hat{V} \simeq g_0 \hat{\beta}_s^\dagger \hat{\beta}_s (\hat{a}_p + \hat{a}_p^\dagger), \quad (6)$$

where $g_0 = -g \sinh(2r_s)$. Here, we have dropped high-frequency components by assuming $\Delta_s \gg \Delta_p$ (see Ref. [50] for a detailed analysis). Equations (5, 6) are reminiscent of the two-tone driven radiation-pressure interaction in cavity optomechanics [63]. Such a radiation-pressure interaction has been applied to implement the steady-state squeezing of mechanical motion [64–69]. In a similar manner, we assume that $\omega_\pm = \Lambda_s \pm \Delta_p$, so that the two-tone driving $\Omega_{2\text{td}}$ is symmetrically detuned from the resonance of the mode $\hat{\beta}_s$. As a result, the signal Bogoliubov mode $\hat{\beta}_s$ is coupled to the pump Bogoliubov mode, $\hat{\beta}_p = \hat{a}_p \cosh(r_p) + \hat{a}_p^\dagger \sinh(r_p)$, through the effective Hamiltonian [50],

$$\hat{H}_{\text{eff}} = \mathcal{G} (\hat{\beta}_p \hat{\beta}_s^\dagger + \hat{\beta}_p^\dagger \hat{\beta}_s). \quad (7)$$

Here, $\tanh(r_p) = G_+/G_-$ and $\mathcal{G} = \sqrt{G_-^2 - G_+^2}$. We have defined $G_\pm = g_0 \alpha_s^\pm$, where α_s^\pm (given in [50]) are the field amplitudes of the mode $\hat{\beta}_s$ induced by the two-tone driving $\Omega_{2\text{td}}$, and for simplicity both have been assumed to be real.

Furthermore, in the limit $r_s \ll 1$, it can be seen that $\mathcal{L}(\hat{a}_s) \hat{\rho} \simeq \mathcal{L}(\hat{\beta}_s) \hat{\rho}$. In such a case, the mode $\hat{\beta}_s$ is equivalently coupled to the vacuum (or zero-temperature) reservoir. Hence, the system dynamics can be described with the effective master equation

$$\dot{\hat{\rho}} = -i [\hat{H}_{\text{eff}}, \hat{\rho}] + \kappa_p \mathcal{L}(\hat{a}_p) \hat{\rho} + \kappa_s \mathcal{L}(\hat{\beta}_s) \hat{\rho}, \quad (8)$$

which means that the Bogoliubov mode $\hat{\beta}_p$ can be cooled by the photon loss of the mode $\hat{\beta}_s$ into its ground state for a large κ_s . This ground state in fact corresponds, in the original laboratory frame, to a squeezed coherent state of the mode \hat{a}_p .

Let us now consider the degree of squeezing. In order to quantify it, we typically use the squeezing parameter [70],

$$\xi_p^2 = 1 + 2 (\langle \hat{a}_p^\dagger \hat{a}_p \rangle - |\langle \hat{a}_p \hat{a}_p \rangle|). \quad (9)$$

Its time evolution is plotted in Fig. 1(b). Specifically, we numerically compare the effective and exact results,

and show an excellent agreement between them. This indicates that the effective master equation in Eq. (8) can be used to predict some larger squeezing by deriving the steady-state squeezing parameter,

$$(\xi_p^2)_{\text{ss}} = \frac{1 + 4\mathcal{C} \exp(-2r_p)}{1 + 4\mathcal{C}}, \quad (10)$$

where $\mathcal{C} = \mathcal{G}^2/(\kappa_s \kappa_p)$ being the cooperativity of the DPA. In Fig. 1(c), $(\xi_p^2)_{\text{ss}}$ is plotted as a function of \mathcal{C} . For realistic parameters of $\kappa_s = 100\kappa_p$, we find that a modest ratio G_+/G_- can keep the steady-state squeezing above 3 dB even for $\mathcal{C} \simeq 0.4$. Moreover, $(\xi_p^2)_{\text{ss}}$ increases as \mathcal{C} , and ultimately reaches its maximum value,

$$(\xi_p^2)_{\text{ss}}^{\text{max}} = \exp(-2r_p) = \frac{1 - G_+/G_-}{1 + G_+/G_-}. \quad (11)$$

For example, with $G_+/G_- = 0.99$, we predict a maximum squeezing of $(\xi_p^2)_{\text{ss}}^{\text{max}} \simeq 23$ dB. Thus by increasing the ratio $G_+/G_- \lesssim 1$, we can, in principle, make intracavity squeezing arbitrarily strong. This is a counterintuitive result from the usual accepted point of view that the steady-state intracavity squeezing of a DPA is theoretically limited to 3 dB.

Enhanced longitudinal qubit readout.—So far, we have demonstrated how to generate a strong cavity-field squeezing in a fully quantum DPA. As a potential application, we show below that this fully-quantum-DPA intracavity squeezing can be used to *exponentially* improve the SNR of longitudinal qubit readout. In the Supplemental Material [50], we analyze the longitudinal readout using intracavity squeezing of a semiclassical DPA. However, we show that this semiclassical-DPA intracavity squeezing *cannot* enable a practically useful increase in the SNR, even with a strong squeezing of the output field.

To begin, we consider the Hamiltonian,

$$\hat{H}_z^{\text{fq}} = \hat{H}_{\text{eff}} + \chi_z \hat{\sigma}_z (\hat{a}_p e^{-i\phi_z} + \hat{a}_p^\dagger e^{i\phi_z}), \quad (12)$$

where $\hat{\sigma}_z$ is the Pauli matrix of the qubit. The first term is used to generate intracavity squeezing, while the second term accounts for the longitudinal qubit-field coupling of strength χ_z and phase ϕ_z . Possible experimental implementations of \hat{H}_z^{fq} are discussed in detail in [50]. Since the photon loss of the mode $\hat{\beta}_s$ is strong, we adiabatically eliminate the mode $\hat{\beta}_s$ to obtain the following equation of motion for the pump mode \hat{a}_p ,

$$\dot{\hat{a}}_p = -i\sigma\chi_z e^{i\phi_z} - \frac{\kappa}{2} \hat{a}_p - \sqrt{\kappa} \hat{\mathcal{A}}_{\text{in}}(t), \quad (13)$$

where $\kappa = \kappa_p^{\text{ad}} + \kappa_p$ is the overall photon loss rate. Here, $\kappa_p^{\text{ad}} = 4\mathcal{G}^2/\kappa_s$ is the rate of the adiabatic photon loss. Moreover, we have defined the overall input noise as $\hat{\mathcal{A}}_{\text{in}}(t) = [\sqrt{\kappa_p^{\text{ad}}} \hat{a}_{p,\text{in}}^{\text{ad}}(t) + \sqrt{\kappa_p} \hat{a}_{p,\text{in}}(t)]/\sqrt{\kappa}$. It involves two uncorrelated noise operators, $\hat{a}_{p,\text{in}}^{\text{ad}}(t)$ and $\hat{a}_{p,\text{in}}(t)$.

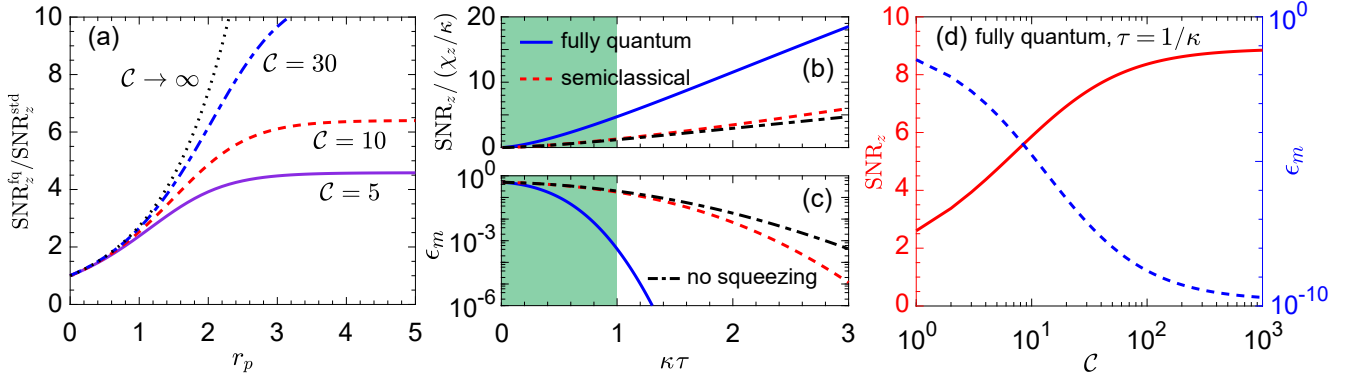


FIG. 2. (a) SNR improvement, i.e., $\text{SNR}_z^{\text{fq}}/\text{SNR}_z^{\text{std}}$, versus the degree r_p of intracavity squeezing for different values of the DPA cooperativity: $C = 5, 10, 30$, and ∞ . An exponential improvement can be obtained for $C \gg \exp(2r_p)/4$. (b) SNR and (c) measurement error as a function of the measurement time. The solid and dashed curves correspond to the longitudinal readout using intracavity squeezing of the fully quantum ($r_p = 2, C = 5$) and semiclassical ($r_{\text{out}}^{\text{sc}} = 2$) DPAs, respectively, while the dash-dotted curves are the results of the standard longitudinal readout with no squeezing. The green shaded area represents the experimentally most interesting regime. In (b) and (c), all parameters are the same except that $\chi_z = \kappa$ in (c). (d) SNR (left axis) and measurement error (right axis) as a function of C in the fully-quantum-DPA case for $\tau = 1/\kappa$. Other parameters are the same as in (c).

The former represents the adiabatic noise arising from the photon loss of the mode $\hat{\beta}_s$, and is given by $i\hat{a}_{p,\text{in}}^{\text{ad}}(t) = \hat{\beta}_{s,\text{in}}(t) \cosh(r_p) + \hat{\beta}_{s,\text{in}}^\dagger(t) \sinh(r_p)$, where $\hat{\beta}_{s,\text{in}}(t)$ is the noise operator of the mode $\hat{\beta}_s$. As mentioned above, $\hat{\beta}_{s,\text{in}}(t)$ can be considered as the vacuum noise in the limit of $r_s \ll 1$, and therefore $\hat{a}_{p,\text{in}}^{\text{ad}}(t)$ corresponds to the squeezed vacuum noise of the mode \hat{a}_p . Moreover, the operator $\hat{a}_{p,\text{in}}(t)$ corresponds to the vacuum noise inducing the natural photon loss of the mode \hat{a}_p .

The longitudinal coupling results in a qubit-state-dependent displacement of the mode \hat{a}_p , and maps the qubit state onto the output quadrature, $\hat{Z}_{\text{out}}(t) = \hat{\mathcal{A}}_{\text{out}}(t)e^{-i\phi_h} + \hat{\mathcal{A}}_{\text{out}}^\dagger(t)e^{i\phi_h}$, which is measured by a homodyne setup with a detection angle ϕ_h . Here, $\hat{\mathcal{A}}_{\text{out}}(t) = \hat{\mathcal{A}}_{\text{in}}(t) + \sqrt{\kappa}\hat{a}_p(t)$ is the overall output field. An essential parameter quantifying the homodyne detection is the SNR, which is evaluated using the operator $\hat{M} = \sqrt{\kappa} \int_0^\tau dt \hat{Z}_{\text{out}}(t)$, with τ the measurement time, and defined as

$$\text{SNR} = \left| \langle \hat{M} \rangle_\uparrow - \langle \hat{M} \rangle_\downarrow \right| \left(\langle \hat{M}_N^2 \rangle_\uparrow + \langle \hat{M}_N^2 \rangle_\downarrow \right)^{-1/2}, \quad (14)$$

where $\{\uparrow, \downarrow\}$ refers to the qubit state. After a straightforward calculation, the SNR of the longitudinal readout using our fully-quantum-DPA intracavity squeezing is given by

$$\text{SNR}_z^{\text{fq}} = \sqrt{\frac{4C + 1}{4C \exp(-2r_p) + 1}} \text{SNR}_z^{\text{std}}, \quad (15)$$

where $\text{SNR}_z^{\text{std}} = 8\chi_z\tau [1 - 2(1 - e^{-\kappa\tau/2})/\kappa\tau] / \sqrt{2\kappa\tau}$ refers to the SNR of the standard longitudinal readout with no squeezing. Equation (15) shows a distinct improvement in the SNR, as in Fig. 2(a). Such an

improvement increases as the cooperativity C , which can, in principle, be made arbitrarily large. Furthermore, as long as $C \gg \exp(2r_p)/4$, we have

$$\text{SNR}_z^{\text{fq}} \simeq \exp(r_p) \text{SNR}_z^{\text{std}}, \quad (16)$$

implying an exponential improvement in the SNR with the degree, r_p , of intracavity squeezing.

More importantly, the SNR improvement, as given in Eqs. (15, 16), holds for *any* measurement time. The reason is that the degree of squeezing of the measurement noise is equal to the degree of intracavity squeezing, i.e., $\langle \hat{M}_N^2 \rangle / \kappa\tau = (\xi_p^2)_{\text{ss}}$, and is independent of the measurement time. This is in stark contrast to the case of using the semiclassical-DPA intracavity squeezing, where, as discussed in [50], the degree of squeezing of the measurement noise increases from the initial value zero, as the measurement time increases, and consequently a large increase in the SNR needs an extremely long measurement time. As illustrated in Fig. 2(a), assuming realistic parameters of $r_p = 2$ ($\simeq 17$ dB) and $C = 5$, our approach gives an approximately four-fold improvement for any measurement time. However, when using the semiclassical-DPA intracavity squeezing, there is almost no improvement for the short-time measurement of most interest in experiments, even though the output-field squeezing, characterized by the parameter $r_{\text{out}}^{\text{sc}} = \ln[(\kappa_s + 4\Omega_{2\text{pd}})/(\kappa_s - 4\Omega_{2\text{pd}})]$, is strong [50].

In Figs. 2(b, c), we plot the SNR and the measurement error, $\epsilon_m = 1 - \mathcal{F}_m$, for the longitudinal readout using the fully-quantum- and semiclassical-DPA intracavity squeezing, and also for the standard longitudinal readout with no squeezing. Here, $\mathcal{F}_m = \frac{1}{2}[1 + \text{erf}(\text{SNR}/2)]$, with erf the error function, is the measurement fidelity. Choosing $r_p = 2$, and $\chi_z = \kappa = 2\pi \times 3$ MHz for our

approach, a short measurement time of $\tau = 1/\kappa \simeq 53$ ns results in $\text{SNR}_z^{\text{fq}} \simeq 4.7$ for $\mathcal{C} = 5$. This corresponds to a measurement error of $\epsilon_m \simeq 4.4 \times 10^{-4}$. When \mathcal{C} increases, as in Fig. 2(d), SNR_z^{fq} can further increase to a maximum of $\simeq 8.9$, and the measurement error rapidly decreases, reaching a minimum of $\simeq 1.5 \times 10^{-10}$. However, at the same measurement time, both the standard longitudinal readout with no squeezing and the case of using the semiclassical-DPA intracavity squeezing enable a much lower SNR, i.e., $\text{SNR}_z^{\text{std}} \simeq \text{SNR}_z^{\text{sc}} \simeq 1.1$, and correspondingly a measurement error of $\simeq 0.22$, which is approximately many orders of magnitude larger.

Conclusions.—We have introduced a method for beating the well-known 3 dB limit of intracavity squeezing of light in a fully quantum DPA. We have demonstrated that an *arbitrary* steady-state squeezing can in principle be achieved for the pump mode, by simply applying a two-tone driving to the signal mode. This counterintuitive intracavity squeezing can *exponentially* increase the SNR of longitudinal qubit readout and, as a result, improve the measurement error by *many orders of magnitude*. In sharp contrast, the semiclassical-DPA intracavity squeezing *cannot* enable a useful increase in the SNR, due to the impractical requirement of a long measurement time. In addition to nondemolition qubit readout, we believe that as an alternative to externally generated and then injected squeezed light, the predicted strong intracavity squeezing could find a wide range of applications.

W.Q. was supported in part by the Incentive Research Project of RIKEN. A.M. was supported by the Polish National Science Centre (NCN) under the Maestro Grant No. DEC-2019/34/A/ST2/00081. F.N. was supported in part by: NTT Research, Army Research Office (ARO) (Grant No. W911NF-18-1-0358), Japan Science and Technology Agency (JST) (via the Q-LEAP program, and the CREST Grant No. JPMJCR1676), Japan Society for the Promotion of Science (JSPS) (via the KAKENHI Grant No. JP20H00134 and the JSPS-RFBR Grant No. JPJSBP120194828), the Asian Office of Aerospace Research and Development (AOARD), and the Foundational Questions Institute Fund (FQXi) via Grant No. FQXi-IAF19-06.

[1] P. D. Drummond and Z. Ficek, *Quantum Squeezing* (Springer, Berlin, 2004).
[2] R. Schnabel, “Squeezed states of light and their applications in laser interferometers,” *Phys. Rep.* **684**, 1–51 (2017).
[3] B. J. Lawrie, P. D. Lett, A. M. Marino, and R. C. Pooser, “Quantum sensing with squeezed light,” *ACS Photonics* **6**, 1307–1318 (2019).
[4] S. L. Braunstein and P. van Loock, “Quantum information with continuous variables,” *Rev. Mod. Phys.*

77, 513–577 (2005).
[5] C. Weedbrook, S. Pirandola, R. García-Patrón, N. J. Cerf, T. C. Ralph, J. H. Shapiro, and S. Lloyd, “Gaussian quantum information,” *Rev. Mod. Phys.* **84**, 621–669 (2012).
[6] J. Abadie *et al.* (LIGO Scientific Collaboration), “A gravitational wave observatory operating beyond the quantum shot-noise limit,” *Nat. Phys.* **7**, 962–965 (2011).
[7] J. Aasi *et al.*, “Enhanced sensitivity of the LIGO gravitational wave detector by using squeezed states of light,” *Nat. Photonics* **7**, 613–619 (2013).
[8] H. Grote, K. Danzmann, K. L. Dooley, R. Schnabel, J. Slutsky, and H. Vahlbruch, “First Long-Term Application of Squeezed States of Light in a Gravitational-Wave Observatory,” *Phys. Rev. Lett.* **110**, 181101 (2013).
[9] M. Asjad, S. Zippilli, and D. Vitali, “Suppression of Stokes scattering and improved optomechanical cooling with squeezed light,” *Phys. Rev. A* **94**, 051801(R) (2016).
[10] J. B. Clark, F. Lecocq, R. W. Simmonds, J. Aumentado, and J. D. Teufel, “Sideband cooling beyond the quantum backaction limit with squeezed light,” *Nature (London)* **541**, 191–195 (2017).
[11] Sh. Barzanjeh, D. P. DiVincenzo, and B. M. Terhal, “Dispersive qubit measurement by interferometry with parametric amplifiers,” *Phys. Rev. B* **90**, 134515 (2014).
[12] N. Didier, A. Kamal, W. D. Oliver, A. Blais, and A. A. Clerk, “Heisenberg-Limited Qubit Read-Out with Two-Mode Squeezed Light,” *Phys. Rev. Lett.* **115**, 093604 (2015).
[13] N. Didier, J. Bourassa, and A. Blais, “Fast Quantum Nondemolition Readout by Parametric Modulation of Longitudinal Qubit-Oscillator Interaction,” *Phys. Rev. Lett.* **115**, 203601 (2015).
[14] L. C. G. Govia and A. A. Clerk, “Enhanced qubit readout using locally generated squeezing and inbuilt Purcell-decay suppression,” *New J. Phys.* **19**, 023044 (2017).
[15] H.-S. Zhong *et al.*, “Quantum computational advantage using photons,” *Science* **370**, 1460–1463 (2020).
[16] H.-S. Zhong *et al.*, “Phase-Programmable Gaussian Boson Sampling Using Stimulated Squeezed Light,” *Phys. Rev. Lett.* **127**, 180502 (2021).
[17] S. Huang and G. S. Agarwal, “Enhancement of cavity cooling of a micromechanical mirror using parametric interactions,” *Phys. Rev. A* **79**, 013821 (2009).
[18] M. Asjad, N. E. Abari, S. Zippilli, and D. Vitali, “Optomechanical cooling with intracavity squeezed light,” *Opt. Express* **27**, 32427–32444 (2019).
[19] H.-K. Lau and A. A. Clerk, “Ground-State Cooling and High-Fidelity Quantum Transduction via Parametrically Driven Bad-Cavity Optomechanics,” *Phys. Rev. Lett.* **124**, 103602 (2020).
[20] X.-Y. Lü, Y. Wu, J. R. Johansson, H. Jing, J. Zhang, and F. Nori, “Squeezed Optomechanics with Phase-Matched Amplification and Dissipation,” *Phys. Rev. Lett.* **114**, 093602 (2015).
[21] S. Zeytinoglu, A. İmamoğlu, and S. Huber, “Engineering Matter Interactions Using Squeezed Vacuum,” *Phys. Rev. X* **7**, 021041 (2017).
[22] W. Qin, A. Miranowicz, P.-B. Li, X.-Y. Lü, J. Q. You, and F. Nori, “Exponentially Enhanced Light-Matter Interaction, Cooperativities, and Steady-State Entanglement Using Parametric Amplification,” *Phys.*

- Rev. Lett. **120**, 093601 (2018).
- [23] C. Leroux, L. C. G. Govia, and A. A. Clerk, “Enhancing Cavity Quantum Electrodynamics via Antisqueezing: Synthetic Ultrastrong Coupling,” *Phys. Rev. Lett.* **120**, 093602 (2018).
- [24] W. Ge, B. C. Sawyer, J. W. Britton, K. Jacobs, J. J. Bollinger, and M. Foss-Feig, “Trapped Ion Quantum Information Processing with Squeezed Phonons,” *Phys. Rev. Lett.* **122**, 030501 (2019).
- [25] P.-B. Li, Y. Zhou, W.-B. Gao, and F. Nori, “Enhancing Spin-Phonon and Spin-Spin Interactions Using Linear Resources in a Hybrid Quantum System,” *Phys. Rev. Lett.* **125**, 153602 (2020).
- [26] S. C. Burd, R. Srinivas, H. M. Knaack, W. Ge, A. C. Wilson, D. J. Wineland, D. Leibfried, J. J. Bollinger, D. T. C. Allcock, and D. H. Slichter, “Quantum amplification of boson-mediated interactions,” *Nat. Phys.* **17**, 898–902 (2021).
- [27] L. Tang, J. Tang, M. Chen, F. Nori, M. Xiao, and K. Xia, “Quantum Squeezing Induced Optical Nonreciprocity,” *Phys. Rev. Lett.* **128**, 083604 (2022).
- [28] A. M. Zagoskin *et al.*, “Controlled Generation of Squeezed States of Microwave Radiation in a Superconducting Resonant Circuit,” *Phys. Rev. Lett.* **101**, 253602 (2008).
- [29] V. Peano, H. G. L. Schwefel, Ch. Marquardt, and F. Marquardt, “Intracavity Squeezing Can Enhance Quantum-Limited Optomechanical Position Detection through Deamplification,” *Phys. Rev. Lett.* **115**, 243603 (2015).
- [30] A. Eddins, J. M. Kreikebaum, D. M. Toyli, E. M. Levenson-Falk, A. Dove, W. P. Livingston, B. A. Levitan, L. C. G. Govia, A. A. Clerk, and I. Siddiqi, “High-Efficiency Measurement of an Artificial Atom Embedded in a Parametric Amplifier,” *Phys. Rev. X* **9**, 011004 (2019).
- [31] L. Krippner, W. J. Munro, and M. D. Reid, “Transient macroscopic quantum superposition states in degenerate parametric oscillation: Calculations in the large-quantum-noise limit using the positive P representation,” *Phys. Rev. A* **50**, 4330–4338 (1994).
- [32] W. J. Munro and M. D. Reid, “Transient macroscopic quantum superposition states in degenerate parametric oscillation using squeezed reservoir fields,” *Phys. Rev. A* **52**, 2388–2391 (1995).
- [33] P. Groszkowski, H.-K. Lau, C. Leroux, L. C. G. Govia, and A. A. Clerk, “Heisenberg-Limited Spin Squeezing via Bosonic Parametric Driving,” *Phys. Rev. Lett.* **125**, 203601 (2020).
- [34] Y.-H. Chen *et al.*, “Shortcuts to Adiabaticity for the Quantum Rabi Model: Efficient Generation of Giant Entangled Cat States via Parametric Amplification,” *Phys. Rev. Lett.* **126**, 023602 (2021).
- [35] P. D. Drummond, K. J. McNeil, and D. F. Walls, “Non-equilibrium Transitions in Sub/second Harmonic Generation,” *Opt. Acta* **28**, 211–225 (1981).
- [36] G. Milburn and D. F. Walls, “Production of squeezed states in a degenerate parametric amplifier,” *Opt. Commun.* **39**, 401–404 (1981).
- [37] M. J. Collett and C. W. Gardiner, “Squeezing of intracavity and traveling-wave light fields produced in parametric amplification,” *Phys. Rev. A* **30**, 1386–1391 (1984).
- [38] N. Didier, F. Qassemi, and A. Blais, “Perfect squeezing by damping modulation in circuit quantum electrodynamics,” *Phys. Rev. A* **89**, 013820 (2014).
- [39] R. Dassonneville, R. Assouly, T. Peronnin, A. A. Clerk, A. Bienfait, and B. Huard, “Dissipative Stabilization of Squeezing Beyond 3 dB in a Microwave Mode,” *PRX Quantum* **2**, 020323 (2021).
- [40] P. Schindler, J. T. Barreiro, T. Monz, V. Nebendahl, D. Nigg, M. Chwalla, M. Hennrich, and R. Blatt, “Experimental repetitive quantum error correction,” *Science* **332**, 1059–1061 (2011).
- [41] J. Kelly *et al.*, “State preservation by repetitive error detection in a superconducting quantum circuit,” *Nature* **519**, 66–69 (2015).
- [42] R. Raussendorf and J. Harrington, “Fault-Tolerant Quantum Computation with High Threshold in Two Dimensions,” *Phys. Rev. Lett.* **98**, 190504 (2007).
- [43] J. M. Gambetta, J. M. Chow, and M. Steffen, “Building logical qubits in a superconducting quantum computing system,” *npj Quantum Inf.* **3**, 2 (2017).
- [44] A. Blais, A. L. Grimsmo, S. M. Girvin, and A. Wallraff, “Circuit quantum electrodynamics,” *Rev. Mod. Phys.* **93**, 025005 (2021).
- [45] P. Krantz, M. Kjaergaard, F. Yan, T. P. Orlando, S. Gustavsson, and W. D. Oliver, “A quantum engineer’s guide to superconducting qubits,” *Appl. Phys. Rev.* **6**, 021318 (2019).
- [46] A. Eddins, S. Schreppler, D. M. Toyli, L. S. Martin, S. Hacohe-Gourgy, L. C. G. Govia, H. Ribeiro, A. A. Clerk, and I. Siddiqi, “Stroboscopic Qubit Measurement with Squeezed Illumination,” *Phys. Rev. Lett.* **120**, 040505 (2018).
- [47] X. Gu, A. F. Kockum, A. Miranowicz, Y.-x. Liu, and F. Nori, “Microwave photonics with superconducting quantum circuits,” *Phys. Rep.* **718–719**, 1–102 (2017).
- [48] S. Touzard, A. Kou, N. E. Frattini, V. V. Sivak, S. Puri, A. Grimm, L. Frunzio, S. Shankar, and M. H. Devoret, “Gated Conditional Displacement Readout of Superconducting Qubits,” *Phys. Rev. Lett.* **122**, 080502 (2019).
- [49] J. Ikonen, J. Goetz, J. Ilves, A. Keränen, A. M. Gunyho, M. Partanen, K. Y. Tan, D. Hazra, L. Grönberg, V. Vesterinen, S. Simbierowicz, J. Hassel, and M. Möttönen, “Qubit Measurement by Multichannel Driving,” *Phys. Rev. Lett.* **122**, 080503 (2019).
- [50] See Supplementary Material, which includes Ref. [71–85], at <http://xxx> for a table containing a summary of our main results, and also for more details about the 3 dB limit of intracavity squeezing, derivation of the effective Hamiltonian for the generation of the strong intracavity squeezing and its interpretation in the laboratory frame, analysis of longitudinal qubit readout using the semiclassical-DPA and fully-quantum-DPA intracavity squeezing, and discussion of a possible implementation of the intracavity-squeezing-enhanced longitudinal qubit readout.
- [51] Z. Leghtas *et al.*, “Confining the state of light to a quantum manifold by engineered two-photon loss,” *Science* **347**, 853 (2015).
- [52] S. Touzard *et al.*, “Coherent Oscillations inside a Quantum Manifold Stabilized by Dissipation,” *Phys. Rev. X* **8**, 021005 (2018).
- [53] R. Lescanne, M. Villiers, T. Peronnin, A. Sarlette, M. Delbecq, B. Huard, T. Kontos, M. Mirrahimi, and Z. Leghtas, “Exponential suppression of bit-flips in a

- qubit encoded in an oscillator,” *Nat. Phys.* **16**, 509 (2020).
- [54] C. W. S. Chang, C. Sabín, P. Forn-Díaz, F. Quijandría, A. M. Vadiraj, I. Nsanzineza, G. Johansson, and C. M. Wilson, “Observation of three-photon spontaneous parametric down-conversion in a superconducting parametric cavity,” *Phys. Rev. X* **10**, 011011 (2020).
- [55] A. Vrajitoarea, Z. Huang, P. Groszkowski, J. Koch, and A. A. Houck, “Quantum control of an oscillator using a stimulated Josephson nonlinearity,” *Nat. Phys.* **16**, 211 (2020).
- [56] X. Guo, C.-L. Zou, and H. X. Tang, “Second-harmonic generation in aluminum nitride microrings with 2500%/W conversion efficiency,” *Optica* **3**, 1126–1131 (2016).
- [57] A. W. Bruch, X. Liu, J. B. Surya, C.-L. Zou, and H. X. Tang, “On-chip $\chi^{(2)}$ microring optical parametric oscillator,” *Optica* **6**, 1361–1366 (2019).
- [58] J.-Q. Wang, Y.-H. Yang, M. Li, X.-X. Hu, J. B. Surya, X.-B. Xu, C.-H. Dong, G.-C. Guo, H. X. Tang, and C.-L. Zou, “Efficient Frequency Conversion in a Degenerate $\chi^{(2)}$ Microresonator,” *Phys. Rev. Lett.* **126**, 133601 (2021).
- [59] M. J. Everitt, T. P. Spiller, G. J. Milburn, R. D. Wilson, and A. M. Zagoskin, “Engineering dissipative channels for realizing Schrödinger cats in SQUIDs,” *Front. ICT* **1**, 1 (2014).
- [60] M. Mirrahimi, Z. Leghtas, V. V. Albert, S. Touzard, R. J. Schoelkopf, L. Jiang, and M. H. Devoret, “Dynamically protected cat-qubits: a new paradigm for universal quantum computation,” *New J. Phys.* **16**, 045014 (2014).
- [61] F.-X. Sun, Q. He, Q. Gong, R. Y. Teh, M. D. Reid, and P. D. Drummond, “Schrödinger cat states and steady states in subharmonic generation with Kerr nonlinearities,” *Phys. Rev. A* **100**, 033827 (2019).
- [62] F.-X. Sun, Q. He, Q. Gong, R. Y. Teh, M. D. Reid, and P. D. Drummond, “Discrete time symmetry breaking in quantum circuits: exact solutions and tunneling,” *New J. Phys.* **21**, 093035 (2019).
- [63] M. Aspelmeyer, T. J. Kippenberg, and F. Marquardt, “Cavity optomechanics,” *Rev. Mod. Phys.* **86**, 1391 (2014).
- [64] A. Kronwald, F. Marquardt, and A. A. Clerk, “Arbitrarily large steady-state bosonic squeezing via dissipation,” *Phys. Rev. A* **88**, 063833 (2013).
- [65] M. J. Woolley and A. A. Clerk, “Two-mode squeezed states in cavity optomechanics via engineering of a single reservoir,” *Phys. Rev. A* **89**, 063805 (2014).
- [66] E. E. Wollman, C. U. Lei, A. J. Weinstein, J. Suh, A. Kronwald, F. Marquardt, A. A. Clerk, and K. C. Schwab, “Quantum squeezing of motion in a mechanical resonator,” *Science* **349**, 952–955 (2015).
- [67] J.-M. Pirkkalainen, E. Damskägg, M. Brandt, F. Massel, and M. A. Sillanpää, “Squeezing of Quantum Noise of Motion in a Micromechanical Resonator,” *Phys. Rev. Lett.* **115**, 243601 (2015).
- [68] C. U. Lei, A. J. Weinstein, J. Suh, E. E. Wollman, A. Kronwald, F. Marquardt, A. A. Clerk, and K. C. Schwab, “Quantum Nondemolition Measurement of a Quantum Squeezed State Beyond the 3 dB limit,” *Phys. Rev. Lett.* **117**, 100801 (2016).
- [69] C. F. Ockeloen-Korppi, E. Damskägg, J.-M. Pirkkalainen, M. Asjad, A. A. Clerk, F. Massel, M. J. Woolley, and M. A. Sillanpää, “Stabilized entanglement of massive mechanical oscillators,” *Nature (London)* **556**, 478 (2018).
- [70] J. Ma, X. Wang, C.-P. Sun, and F. Nori, “Quantum spin squeezing,” *Phys. Rep.* **509**, 89 (2011).
- [71] O. Gamel and D. F. V. James, “Time-averaged quantum dynamics and the validity of the effective Hamiltonian model,” *Phys. Rev. A* **82**, 052106 (2010).
- [72] C. W. Gardiner and M. J. Collett, “Input and output in damped quantum systems: Quantum stochastic differential equations and the master equation,” *Phys. Rev. A* **31**, 3761–3774 (1985).
- [73] X. Wang, A. Miranowicz, and F. Nori, “Ideal Quantum Nondemolition Readout of a Flux Qubit without Purcell Limitations,” *Phys. Rev. Applied* **12**, 064037 (2019).
- [74] I. Strandberg, G. Johansson, and F. Quijandría, “Wigner negativity in the steady-state output of a Kerr parametric oscillator,” *Phys. Rev. Research* **3**, 023041 (2021).
- [75] Y. Lu, I. Strandberg, F. Quijandría, G. Johansson, S. Gasparinetti, and P. Delsing, “Propagating Wigner-Negative States Generated from the Steady-State Emission of a Superconducting Qubit,” *Phys. Rev. Lett.* **126**, 253602 (2021).
- [76] Y.-x. Liu *et al.*, “Controllable Coupling between Flux Qubits,” *Phys. Rev. Lett.* **96**, 067003 (2006).
- [77] A. J. Kerman, “Quantum information processing using quasiclassical electromagnetic interactions between qubits and electrical resonators,” *New J. Phys.* **15**, 123011 (2013).
- [78] P.-M. Billangeon, J. S. Tsai, and Y. Nakamura, “Circuit-QED-based scalable architectures for quantum information processing with superconducting qubits,” *Phys. Rev. B* **91**, 094517 (2015).
- [79] P.-M. Billangeon, J. S. Tsai, and Y. Nakamura, “Scalable architecture for quantum information processing with superconducting flux qubits based on purely longitudinal interactions,” *Phys. Rev. B* **92**, 020509(R) (2015).
- [80] S. Richer and D. DiVincenzo, “Circuit design implementing longitudinal coupling: A scalable scheme for superconducting qubits,” *Phys. Rev. B* **93**, 134501 (2016).
- [81] S. Richer, N. Maleeva, S. T. Skacel, I. M. Pop, and D. DiVincenzo, “Inductively shunted transmon qubit with tunable transverse and longitudinal coupling,” *Phys. Rev. B* **96**, 174520 (2017).
- [82] R. Stassi and F. Nori, “Long-lasting quantum memories: Extending the coherence time of superconducting artificial atoms in the ultrastrong-coupling regime,” *Phys. Rev. A* **97**, 033823 (2018).
- [83] J. Q. You and F. Nori, “Quantum information processing with superconducting qubits in a microwave field,” *Phys. Rev. B* **68**, 064509 (2003).
- [84] A. Blais, J. Gambetta, A. Wallraff, D. I. Schuster, S. M. Girvin, M. H. Devoret, and R. J. Schoelkopf, “Quantum-information processing with circuit quantum electrodynamics,” *Phys. Rev. A* **75**, 032329 (2007).
- [85] R. Dassonneville *et al.*, “Fast High-Fidelity Quantum Nondemolition Qubit Readout via a Nonperturbative Cross-Kerr Coupling,” *Phys. Rev. X* **10**, 011045 (2020).

SUPPLEMENTAL MATERIAL

Introduction

Here, we first summarize our main results in this work. Next, we recall the 3 dB limit of intracavity squeezing of the semiclassical degenerate parametric amplifier (DPA) to explain the reason for that limit. Subsequently, we present a detailed derivation of the effective Hamiltonian used to generate a strong steady-state intracavity squeezing, and then discuss its physical interpretation in the laboratory frame. Furthermore, we analyze the effects of intracavity squeezing of the semiclassical and fully quantum DPAs on longitudinal qubit readout. Finally, a possible implementation of our proposal for the intracavity-squeezing enhanced longitudinal qubit readout is discussed.

S1. Summary of our main results

Before discussing more technical details about our work, we first summarize the main results of this work in this section. These results, including some numerical values, are summarized in Table I by comparing intracavity squeezing of the semiclassical and fully quantum DPAs and their effects on longitudinal qubit readout. More details of our main results are described as follows:

- (1) While intracavity squeezing of the semiclassical DPA is limited, as is well known, to at most 3 dB, we show that our approach can, in principle, lead to an arbitrarily strong intracavity squeezing by exploiting the pump mode of a fully quantum DPA.

The reason for this sharp contrast is that the photon loss of the signal mode, which is the origin of the 3 dB squeezing limit of the semiclassical DPA, is now engineered as a resource in our approach rather than a noise source.

- (2) Furthermore, the strong fully-quantum-DPA intracavity squeezing, which is equivalent to an externally generated and injected squeezed reservoir, is applied to longitudinal qubit readout. For comparison, we also analyze the effect of the semiclassical-DPA intracavity squeezing on such a readout. We find that these two types of intracavity squeezing exhibit strikingly different performances.

In the semiclassical-DPA case, we find that the degree of squeezing of the measurement noise strongly depends on the measurement time, i.e., it increases from zero as the measurement time increases. This means that a large squeezing of the measurement noise, corresponding to a high readout SNR, needs a long measurement time. Thus,

TABLE I. Comparison between intracavity squeezing of the semiclassical and fully quantum DPAs, and between their effects on longitudinal qubit readout. Here, \mathcal{C} is the cooperativity of the fully quantum DPA, SNR stands for the signal-to-noise ratio, $\text{SNR}_z^{\text{std}}$ is the SNR of the standard longitudinal readout with no squeezing, ϵ_m is the measurement error, τ is the measurement time, r_p is the degree of intracavity squeezing of the fully quantum DPA, and $r_{\text{out}}^{\text{sc}}$ is the degree of squeezing of the output field of the semiclassical DPA.

DPA type	Steady-state intracavity squeezing	Longitudinal qubit readout					
		\mathcal{C}	$\text{SNR}/\text{SNR}_z^{\text{std}}$	SNR^{\S}	ϵ_m	τ (ns)	Degree of squeezing of the measurement noise
semiclassical	at most 3 dB	—	$\simeq 1^\dagger$	1.1	$\simeq 0.22$	$\simeq 53$	τ -dependent
fully quantum	arbitrarily strong	any	$\sqrt{\frac{4\mathcal{C}+1}{4\mathcal{C}\exp(-2r_p)+1}}$	4.7	$\simeq 4.4 \times 10^{-4}$		τ -independent
		$\gg \frac{1}{4}\exp(2r_p)$	$\simeq \exp(r_p)$	8.9	$\simeq 1.5 \times 10^{-10}$		

[†] This case of effectively no improvement is observed even for a large $r_{\text{out}}^{\text{sc}}$;

[§] To calculate the SNR values, we assume $r_{\text{out}}^{\text{sc}} = r_p = 2$ ($\simeq 17$ dB), and a modest cooperativity of $\mathcal{C} = 5$.

the semiclassical-DPA intracavity squeezing cannot enable a significant increase in the SNR for the short-time measurement of practical interest, even with a strong squeezing of the output field. However, this is not the case when our fully-quantum-DPA intracavity squeezing is used.

We demonstrate that in the fully-quantum-DPA case, the degree of squeezing of the measurement noise is equal to the degree of intracavity squeezing, and is independent of the measurement time. This enables an exponential increase in the SNR for any measurement time, and leads to an extremely low measurement error, which can be made many orders of magnitude smaller than those obtained in both the semiclassical-DPA case and the standard longitudinal readout with no squeezing.

Having summarized the main results presented in our work, we show more technical details in the following sections.

S2. Limited steady-state intracavity squeezing of the semiclassical degenerate parametric amplifier

In this section, we recall the 3 dB limit of the semiclassical-DPA intracavity squeezing, and give the reason for such a limit, i.e., the photon loss of the signal mode. We begin with the standard master equation,

$$\dot{\hat{\rho}}_s = -i \left[\hat{H}_{2\text{pd}}, \hat{\rho}_s \right] + \kappa_s \mathcal{L}(\hat{a}_s) \hat{\rho}_s, \quad (\text{S1})$$

where

$$\hat{H}_{2\text{pd}} = \Delta_s \hat{a}_s^\dagger \hat{a}_s + \Omega_{2\text{pd}} (\hat{a}_s^2 + \text{H.c.}), \quad (\text{S2})$$

and $\hat{\rho}_s$ is the density matrix of the signal mode \hat{a}_s . Under the master equation, the number of intracavity photons, $\langle \hat{a}_s^\dagger \hat{a}_s \rangle$, and the two-photon-correlation term, $\langle \hat{a}_s \hat{a}_s \rangle$, evolve as

$$\langle \hat{a}_s^\dagger \hat{a}_s \rangle(t) = \frac{8\Omega_{2\text{pd}}^2}{\kappa_s^2 - 4\omega^2} - \mathcal{Q}_0 \exp(-\kappa_s t), \quad (\text{S3})$$

$$\langle \hat{a}_s \hat{a}_s \rangle(t) = -\frac{2\Omega(2\Delta_s + i\kappa_s)}{\kappa_s^2 - 4\omega^2} + \mathcal{Q}_1 \exp(-\kappa_s t), \quad (\text{S4})$$

where $\omega = \sqrt{4\Omega_{2\text{pd}}^2 - \Delta_s^2}$, and we have defined

$$\mathcal{Q}_0 = \frac{4\Omega_{2\text{pd}}^2}{\omega(\kappa_s^2 - 4\omega^2)} [2\omega \cosh(2\omega t) + \kappa_s \sinh(2\omega t)], \quad (\text{S5})$$

$$\mathcal{Q}_1 = \frac{2\Omega}{\omega(\kappa_s^2 - 4\omega^2)} [\omega(2\Delta_s + i\kappa_s) \cosh(2\omega t) - (i2\Delta_s^2 - \Delta_s \kappa_s - i8\Omega_{2\text{pd}}^2) \sinh(2\omega t)]. \quad (\text{S6})$$

To ensure that the system is stable, ω is required to be either a purely imaginary number, or a purely real number but smaller than $\kappa_s/2$. As a consequence, the squeezing parameter,

$$\xi_s^2 = 1 + 2(\langle \hat{a}_s^\dagger \hat{a}_s \rangle - |\langle \hat{a}_s \hat{a}_s \rangle|), \quad (\text{S7})$$

in the steady state ($t \rightarrow \infty$) is found to be

$$(\xi_s^2)_{\text{ss}} = \frac{1}{1 + \epsilon}, \quad (\text{S8})$$

where

$$\epsilon = \frac{4\Omega_{2\text{pd}}^2}{\sqrt{\kappa_s^2 - 4\omega^2} + (4\Omega_{2\text{pd}}^2)^2}. \quad (\text{S9})$$

It is clear that $\epsilon > 1$, and thus that as shown in Fig. S1, the maximum $(\xi_s^2)_{\text{ss}}$ is limited to 0.5, corresponding to 3 dB. This squeezing limit is attributed to the photon loss of the signal mode, because it destroys two-photon correlations [represented by the term $\langle \hat{a}_s \hat{a}_s \rangle$ in Eq. (S7)], which play a key role in the formation of squeezing. However, in the present work, we demonstrate that this photon loss of the signal mode, when exploited as a resource via quantum reservoir engineering, can cause an arbitrarily strong steady-state squeezing for a quantized pump mode of the DPA.

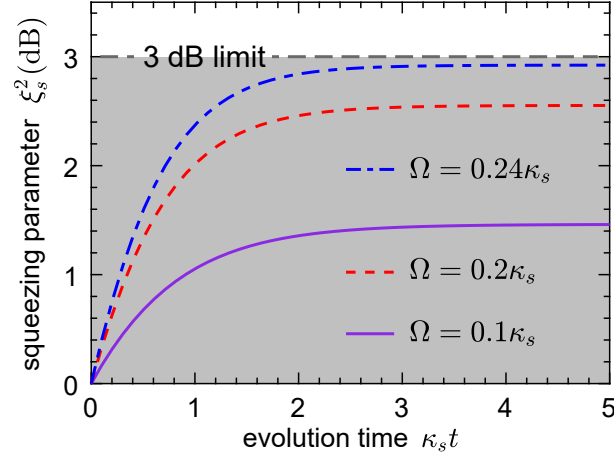


FIG. S1. Upper-bounded steady-state intracavity squeezing of the semiclassical degenerate parametric amplifier. Here, we set $\Delta_s = 0$ as an example, so that the steady-state squeezing of the signal mode \hat{a}_s approaches 3 dB as $\Omega_{2\text{pd}} \rightarrow \kappa_s/4$. The gray shaded area refers to the regime below the 3 dB limit. Note that when $\Omega_{2\text{pd}} > \kappa_s/4$, the system becomes unstable.

S3. Detailed derivation of the effective Hamiltonian \hat{H}_{eff}

Below, we give a detailed derivation of the effective Hamiltonian \hat{H}_{eff} to implement a strong steady-state intracavity squeezing of light. To begin, we consider the original Hamiltonian $\hat{H} = \hat{H}_0 + \hat{H}_{2\text{td}}$, where \hat{H}_0 and $\hat{H}_{2\text{td}}$ are given in Eqs. (1) and (2), respectively, in the main article. In terms of the signal Bogoliubov mode $\hat{\beta}_s$, the Hamiltonian \hat{H} is reexpressed as

$$\hat{H} = \hat{\mathcal{H}} + \hat{R}_1 + \hat{R}_1^\dagger + \hat{R}_2 + \hat{R}_2^\dagger, \quad (\text{S10})$$

$$\begin{aligned} \hat{\mathcal{H}} = & \Delta_p \hat{a}_p^\dagger \hat{a}_p + \Lambda_s \hat{\beta}_s^\dagger \hat{\beta}_s + g_0 \hat{\beta}_s^\dagger \hat{\beta}_s (\hat{a}_p + \hat{a}_p^\dagger) \\ & + \cosh(r_s) \sum_{k=\pm} \left(\mathcal{E}_k \hat{\beta}_s^\dagger e^{-i\omega_k t} + \text{H.c.} \right), \end{aligned} \quad (\text{S11})$$

$$\hat{R}_1 = g \left[\cosh^2(r_s) \hat{\beta}_s^2 + \sinh^2(r_s) \hat{\beta}_s^{\dagger 2} \right] \hat{a}_p^\dagger, \quad (\text{S12})$$

$$\hat{R}_2 = -\sinh(r_s) \sum_{k=\pm} \mathcal{E}_k \hat{\beta}_s e^{-i\omega_k t}. \quad (\text{S13})$$

Here, \hat{R}_1 and \hat{R}_2 are the residual components of the parametric coupling g and the two-tone driving $\Omega_{2\text{td}}$, respectively. Correspondingly, the master equation is given by

$$\begin{aligned} \dot{\hat{\rho}} = & -i \left[\hat{H}, \hat{\rho} \right] + \kappa_p \mathcal{L}(\hat{a}_p) \hat{\rho} + \kappa_s \cosh^2(r_s) \mathcal{L}(\hat{\beta}_s) \hat{\rho} \\ & + \kappa_s \sinh^2(r_s) \mathcal{L}(\hat{\beta}_s^\dagger) \hat{\rho} - \frac{1}{2} \kappa_s \sinh(2r_s) \mathcal{D}(\hat{\beta}_s) \hat{\rho} \\ & - \frac{1}{2} \kappa_s \sinh(2r_s) \mathcal{D}(\hat{\beta}_s^\dagger) \hat{\rho}. \end{aligned} \quad (\text{S14})$$

In order to derive the Hamiltonian \hat{H}_{eff} , we perform four steps (see below). In these steps, let us first focus our attention on the term $\hat{\mathcal{H}}$, which makes the dominant contribution to the generation of intracavity squeezing. We then analyze the terms \hat{R}_1 and \hat{R}_2 , both of which, as purely high-frequency effects, can be dropped by properly compensating some resonance shifts of the modes $\hat{\beta}_s$ and \hat{a}_p . Note that the rotating frames mentioned in Steps (1)–(3) are relative to the frame, which the Hamiltonian \hat{H} in Eq. (S10) is in.

- (1) Let us first work in the rotating frame of reference of $\hat{h}_1 = \omega_- \hat{\beta}_s^\dagger \hat{\beta}_s$, and make a displacement transformation for the mode $\hat{\beta}_s$, i.e., $\hat{\beta}_s \rightarrow \hat{\beta}_s + \alpha_s^-$ and also for the mode \hat{a}_p , i.e., $\hat{a}_p \rightarrow \hat{a}_p + \alpha_p^-$. Here, α_s^- and α_p^- are the field

amplitudes of the modes $\hat{\beta}_s$ and \hat{a}_p , respectively, which are induced by the ω_- driving tone. Set

$$\alpha_p^- = \frac{g_0 |\alpha_s^-|^2}{i\kappa_p/2 - \Delta_p}, \quad (\text{S15})$$

$$\alpha_s^- = \frac{\cosh(r_s) \mathcal{E}_-}{i\kappa_s/2 - \Lambda_s - \delta_- + \omega_-}, \quad (\text{S16})$$

where $\delta_- = 2g_0 \text{Re}[\alpha_p^-]$ is a resonance shift of the mode $\hat{\beta}_s$ induced by the ω_- driving tone. Then returning to the original frame, it is seen that $\hat{\mathcal{H}}$ is transformed to

$$\begin{aligned} \hat{\mathcal{H}}_- &= \Delta_p \hat{a}_p^\dagger \hat{a}_p + (\Lambda_s + \delta_-) \hat{\beta}_s^\dagger \hat{\beta}_s + g_0 \hat{\beta}_s^\dagger \hat{\beta}_s (\hat{a}_p + \hat{a}_p^\dagger) \\ &\quad + g_0 \left(\alpha_s^- \hat{\beta}_s^\dagger e^{-i\omega_- t} + \text{H.c.} \right) (\hat{a}_p + \hat{a}_p^\dagger) \\ &\quad + \cosh(r_s) \mathcal{E}_+ \hat{\beta}_s^\dagger e^{-i\omega_+ t} + \text{H.c.} \end{aligned} \quad (\text{S17})$$

- (2) Having obtained $\hat{\mathcal{H}}_-$, we enter the rotating frame of reference of $\hat{h}_2 = \omega_+ \hat{\beta}_s^\dagger \hat{\beta}_s$, and make the displacement transformations for the modes $\hat{\beta}_s$ and \hat{a}_p , i.e., $\hat{\beta}_s \rightarrow \hat{\beta}_s + \alpha_s^+$ and $\hat{a}_p \rightarrow \hat{a}_p + \alpha_p^+$. Here, α_s^+ and α_p^+ are the field amplitudes of the modes $\hat{\beta}_s$ and \hat{a}_p , respectively, which are induced by the ω_+ driving tone. Set

$$\alpha_p^+ = \frac{g_0 |\alpha_s^+|^2}{i\kappa_p/2 - \Delta_p}, \quad (\text{S18})$$

$$\alpha_s^+ = \frac{\cosh(r_s) \mathcal{E}_+}{i\kappa_s/2 - \Lambda_s - \delta_- - \delta_+ + \omega_+}, \quad (\text{S19})$$

where $\delta_+ = 2g_0 \text{Re}[\alpha_p^+]$ is a resonance shift of the mode $\hat{\beta}_s$ induced by the ω_+ driving tone. Then returning to the original frame, it is seen that $\hat{\mathcal{H}}_-$ is transformed to

$$\begin{aligned} \hat{\mathcal{H}}_+ &= \Delta_p \hat{a}_p^\dagger \hat{a}_p + \Lambda_s \hat{\beta}_s^\dagger \hat{\beta}_s + g_0 \hat{\beta}_s^\dagger \hat{\beta}_s (\hat{a}_p + \hat{a}_p^\dagger) \\ &\quad + g_0 \left(\alpha_s^+ \hat{\beta}_s^\dagger e^{-i\omega_+ t} + \text{H.c.} \right) (\hat{a}_p + \hat{a}_p^\dagger) + g_0 \left(\alpha_s^- \hat{\beta}_s^\dagger e^{-i\omega_- t} + \text{H.c.} \right) (\hat{a}_p + \hat{a}_p^\dagger) \\ &\quad + g_0 \left[\alpha_s^- (\alpha_s^+)^* e^{-i(\omega_- - \omega_+)t} + \text{H.c.} \right] (\hat{a}_p + \hat{a}_p^\dagger) + 2g_0 \text{Re}[\alpha_p^+] \left(\alpha_s^- \hat{\beta}_s^\dagger e^{-i\omega_- t} + \text{H.c.} \right), \end{aligned} \quad (\text{S20})$$

where the overall resonance shift, $\delta_- + \delta_+$, of the mode $\hat{\beta}_s$ has been absorbed into Λ_s .

- (3) Assume that $\omega_\pm = \Lambda_s \pm \Delta_p$, and transform $\hat{\mathcal{H}}_+$ into the rotating frame of reference of $\hat{h}_3 = \Delta_p \hat{a}_p^\dagger \hat{a}_p + \Lambda_s \hat{\beta}_s^\dagger \hat{\beta}_s$. Then dropping high-frequency components yields

$$\hat{H}_{\text{eff}} = g_0 \left(\alpha_s^- \hat{\beta}_s^\dagger \hat{a}_p + \alpha_s^+ \hat{\beta}_s^\dagger \hat{a}_p^\dagger + \text{H.c.} \right) \quad (\text{S21})$$

$$= \mathcal{G} \left(\hat{\beta}_p \hat{\beta}_s^\dagger + \hat{\beta}_p^\dagger \hat{\beta}_s \right), \quad (\text{S22})$$

where we have set the field amplitudes α_s^\pm to be real for simplicity.

- (4) Now consider the terms \hat{R}_1 and \hat{R}_2 . We follow the same procedures as given in Steps (1) and (2), and see that \hat{R}_{1+} becomes

$$\hat{R}_{1+} = g \left[\cosh^2(r_s) \hat{\Pi} + \sinh^2(r_s) \hat{\Pi}^\dagger \right] \left[\hat{a}_p^\dagger + (\alpha_p^-)^* + (\alpha_p^+)^* \right], \quad (\text{S23})$$

with

$$\hat{\Pi} = \hat{\beta}_s^2 + 2\hat{\beta}_s \sum_{k=\pm} \alpha_s^k e^{-i\omega_k t} + \left(\sum_{k=\pm} \alpha_s^k e^{-i\omega_k t} \right)^2. \quad (\text{S24})$$

As assumed in the main article, the degree, r_s , of squeezing of the signal mode \hat{a}_s is very small, so that the terms in Eq. (S23), which are proportional to $\sinh^2(r_s)$, can be dropped, yielding

$$\hat{R}_{1+} \simeq g_c \hat{\Pi} \left[\hat{a}_p^\dagger + (\alpha_p^-)^* + (\alpha_p^+)^* \right] + \text{H.c.}, \quad (\text{S25})$$

where $g_c = g \cosh^2(r_s) \simeq g$. The coupling \hat{R}_{1+} is dominated by the couplings,

$$\hat{P} = 2g_c \hat{\beta}_s a_p^\dagger \sum_{k=\pm} \alpha_s^k e^{-i\omega_k t} + \text{H.c.}, \quad (\text{S26})$$

$$\hat{Q} = g_c \left(\sum_{k=\pm} \alpha_s^k e^{-i\omega_k t} \right)^2 \hat{a}_p^\dagger + \text{H.c.} \quad (\text{S27})$$

Using the formalism of Ref. [S1] shows that, under the resonance conditions $\omega_{\pm} = \Lambda_s \pm \Delta_p$, the dynamics of the coupling \hat{P} effectively causes a resonance up-shift of

$$\delta_{\text{shift}} = 2g_c^2 \left[\frac{1}{\Lambda_s} (\alpha_s^+)^2 + \frac{1}{\Lambda_s - \Delta_p} (\alpha_s^-)^2 \right] \quad (\text{S28})$$

for the mode $\hat{\beta}_s$, and also a resonance down-shift of the same amount for the mode \hat{a}_p . These two shifts can be compensated by slightly modifying the resonance condition $\omega_- = \Lambda_s - \Delta_p$ to be $\omega_- = \Lambda_s - \Delta_p + 2\delta_{\text{shift}}$.

On the other hand, the coupling \hat{Q} can be simply viewed as a detuned three-tone driving of the mode \hat{a}_p . To cancel its effect, a direct method is to drive the mode \hat{a}_p using another opposite-phase three-tone driving. But to simplify this problem, we note that recently, a strong single-photon parametric coupling has been experimentally realized, with the strength g being able to range from some tens of kHz to some tens of MHz [S2–S9]. This indicates that even when the intracavity-field amplitudes α_s^{\pm} are small [e.g., $\alpha_s^{\pm} \sim 1$ as in Fig. 1(b)], a large \mathcal{C} can still be achieved. Here, $\mathcal{C} = g^2 \sinh^2(2r_s) \left[(\alpha_s^-)^2 - (\alpha_s^+)^2 \right] / (\kappa_s \kappa_p)$ is a key factor, whose larger value can lead to a stronger intracavity squeezing as discussed in the main article. Thus in this case, the coupling \hat{Q} acts as a high-frequency component. At the same time, the residual driving term \hat{R}_2 can also be treated as a high-frequency component, because for $r_s \ll 1$ we can have $(\omega_{\pm} + \Lambda_s) \gg \sinh(r_s) \mathcal{E}_{\pm}$. Consequently, both the terms \hat{Q} and \hat{R}_2 are allowed to be directly dropped. Such is the case considered in the main article.

By the detailed analysis in the four steps above, it is seen that the coherent dynamics of the three-tone driven DPA, which is described exactly by the Hamiltonian \hat{H} , can be well governed by the effective Hamiltonian \hat{H}_{eff} . This is numerically confirmed in Fig. 1(b) in the main article.

S4. Physical interpretation of the Hamiltonian \hat{H}_{eff} in the laboratory frame

The effective Hamiltonian \hat{H}_{eff} models a beam-splitter-type interaction between the signal and pump Bogoliubov modes, but *in the squeezed frame*. Below, we discuss how to understand this effective Hamiltonian *in the laboratory frame*. To be more specific, we first note that the signal Bogoliubov mode $\hat{\beta}_s$ in the squeezed frame, whose resonance frequency is $\Lambda_s = \sqrt{\Delta_s^2 - 4\Omega_{2\text{pd}}^2}$, in fact corresponds to the shifted (or dressed) signal mode in the laboratory frame, whose resonance frequency is $\omega_s^{\text{sq}} = \omega_d/2 + \Lambda_s$. In the laboratory frame, \hat{H}_{eff} can be rewritten as

$$\hat{H}_{\text{eff}} = \hat{H}_{\text{BST}} + \hat{H}_{\text{TMS}}, \quad (\text{S29})$$

$$\hat{H}_{\text{BST}} = G_- \left(\hat{a}_p \hat{\beta}_s^\dagger + \hat{a}_p^\dagger \hat{\beta}_s \right), \quad (\text{S30})$$

$$\hat{H}_{\text{TMS}} = G_+ \left(\hat{a}_p \hat{\beta}_s + \hat{a}_p^\dagger \hat{\beta}_s^\dagger \right). \quad (\text{S31})$$

Here, \hat{H}_{BST} and \hat{H}_{TMS} describe a resonant beam-splitter-type interaction and a resonant two-mode-squeezing interaction, respectively. Thus, the physical interpretation of \hat{H}_{eff} can be understood as two four-wave-mixing processes, as schematically depicted in Fig. S2.

The beam-splitter-type interaction \hat{H}_{BST} in Eq. (S30) exchanges a single photon between the signal Bogoliubov mode $\hat{\beta}_s$ at ω_s^{sq} and the pump mode \hat{a}_p at ω_p . This process is obtained under the resonance condition $\omega_- = \Lambda_s - \Delta_p$, which, in the laboratory frame, is

$$\omega_-^{\text{d}} + \omega_p = \omega_s^{\text{sq}} + \omega_d. \quad (\text{S32})$$

It is seen that the beam-splitter-type interaction \hat{H}_{BST} originates from a four-wave-mixing process, which is stimulated by the driving tones at ω_-^{d} and ω_d . According to the photon description of this process [see Fig. S2(a)], a pump photon

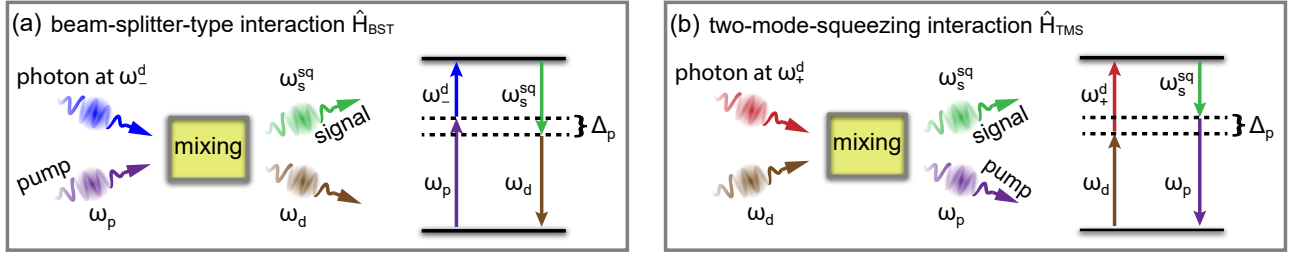


FIG. S2. Four-wave-mixing processes responsible for (a) the beam-splitter-type [i.e., \hat{H}_{BST} in Eq. (S30)] and (b) two-mode-squeezing [i.e., \hat{H}_{TMS} in Eq. (S31)] interactions in the laboratory frame. On the right of both panels is the schematic representation of energy conservation showing the resonance conditions of these interactions, $\omega_{\pm} = \Lambda_{\pm} \pm \Delta_p$. The beam-splitter-type interaction models the conversion of a photon from the pump mode \hat{a}_p at ω_p into the signal Bogoliubov mode (i.e., the shifted signal mode) $\hat{\beta}_s$ at ω_s^{sq} , which is accompanied by absorbing an ω_d^{d} photon and emitting another ω_d photon. In contrast, the two-mode-squeezing interaction models the simultaneous creation of two photons in the signal Bogoliubov and pump modes, along with the simultaneous annihilation of an ω_+^{d} photon and an ω_d photon.

at ω_p is down-converted to the mode $\hat{\beta}_s$ at ω_s^{sq} , while annihilating a driving photon at ω_+^{d} and creating another driving photon at ω_d .

On the other hand, the two-mode-squeezing interaction \hat{H}_{TMS} in Eq. (S31) describes the simultaneous annihilation and creation of two photons in the signal Bogoliubov mode $\hat{\beta}_s$ and the pump mode \hat{a}_p . Its resonance condition is $\omega_+ = \Lambda_s + \Delta_p$, which, in the laboratory frame, reads

$$\omega_+^{\text{d}} + \omega_d = \omega_s^{\text{sq}} + \omega_p. \quad (\text{S33})$$

This implies that the driving tones at ω_+^{d} and ω_d simulate a four-wave-mixing process [see Fig. S2(b)]. In the photon description, a photon pair of the signal Bogoliubov and pump modes can be created by annihilating two driving photons at ω_+^{d} and ω_d .

S5. Longitudinal qubit readout using the semiclassical-DPA intracavity squeezing

In this section, we consider the longitudinal readout of a qubit embedded in the semiclassical DPA, where the pump mode is treated as a classical field and, in turn, as a nonlinear two-photon driving of the signal mode. Specifically, we derive and analyze in detail the measurement signal, measurement noise, and SNR. For a semiclassical DPA, its intracavity squeezing is limited to 3 dB, but at the same time an arbitrarily strong squeezing can, in principle, be achieved for its output field. It thus seems, at first glance, as though the semiclassical-DPA intracavity squeezing might be suitable to improve longitudinal qubit readout. However, below we demonstrate that *for the short-time measurement, the SNR does not benefit from the semiclassical-DPA intracavity squeezing, even though squeezing of the output field is very strong*. Furthermore, we also demonstrate that *although there is an exponential improvement in the SNR for the long-time measurement, the required measurement time is extremely long and, therefore, is infeasible experimentally*.

To begin, we assume that the qubit to be measured is longitudinally coupled to the signal mode \hat{a}_s , as described by the Hamiltonian,

$$\hat{H}_z^{\text{sc}} = \Omega_{2\text{pd}} (\hat{a}_s^2 e^{-i2\phi_{2\text{pd}}} + \hat{a}_s^{\dagger 2} e^{i2\phi_{2\text{pd}}}) + \chi_z \hat{\sigma}_z (\hat{a}_s e^{-i\phi_z} + \hat{a}_s^{\dagger} e^{i\phi_z}), \quad (\text{S34})$$

where $\hat{\sigma}_z$ is the Pauli matrix of the qubit. The first term accounts for the semiclassical DPA with a two-photon driving of strength $\Omega_{2\text{pd}}$ and phase $2\phi_{2\text{pd}}$, and the second term for the longitudinal qubit-field coupling of strength χ_z and phase ϕ_z . The longitudinal coupling generates a linear displacement of the signal mode \hat{a}_s , conditional on the qubit state. Under \hat{H}_z^{sc} , the quantum Langevin equation of motion for the signal mode \hat{a}_s is

$$\dot{\hat{a}}_s = -i\sigma\chi_z e^{i\phi_z} - \frac{\kappa_s}{2}\hat{a}_s - i2\Omega_{2\text{pd}}\hat{a}_s^{\dagger} e^{i2\phi_{2\text{pd}}} - \sqrt{\kappa_s}\hat{a}_{s,\text{in}}(t). \quad (\text{S35})$$

Here, the qubit has been assumed to be in a definite state, such that the operator $\hat{\sigma}_z$ has been written as a c-number $\sigma = \pm 1$, corresponding to the excited and ground states of the qubit, respectively. This equation of motion can be

solved using a formal integration, and the resulting expression for $\hat{a}_s(t)$ is

$$\begin{aligned}\hat{a}_s(t) = & \cosh[2\Omega_{2\text{pd}}(t-t_0)]\hat{a}_s(t_0)e^{-\kappa_s(t-t_0)/2} \\ & - ie^{i2\phi_{2\text{pd}}}\sinh[2\Omega_{2\text{pd}}(t-t_0)]\hat{a}_s^\dagger(t_0)e^{-\kappa_s(t-t_0)/2} \\ & - \sqrt{\kappa_s}\int_{t_0}^t ds \cosh[2\Omega_{2\text{pd}}(t-s)]\left[\hat{a}_{s,\text{in}}(t) + ie^{i\phi_z}\sigma\chi_z/\sqrt{\kappa_s}\right]e^{-\kappa_s(t-s)/2} \\ & + ie^{i2\phi_{2\text{pd}}}\sqrt{\kappa_s}\int_{t_0}^t ds \sinh[2\Omega_{2\text{pd}}(t-s)]\left[\hat{a}_{s,\text{in}}^\dagger(t) - ie^{-i\phi_z}\sigma\chi_z/\sqrt{\kappa_s}\right]e^{-\kappa_s(t-s)/2},\end{aligned}\quad (\text{S36})$$

where t_0 is the initial time of the measurement. It is seen that in the case of $\Omega_{2\text{pd}} > \kappa_s/4$, the amplitude of \hat{a}_s increases exponentially with time, and the system becomes unstable. Thus, in order for the system to be stable, we restrict our discussion to the case where $\Omega_{2\text{pd}} < \kappa_s/4$. Note that the special case of $\Omega_{2\text{pd}} = 0$ corresponds to the standard longitudinal readout with no squeezing.

With the output field $\hat{a}_{s,\text{out}}(t) = \hat{a}_{s,\text{in}}(t) + \sqrt{\kappa_s}\hat{a}_s(t)$ [S10], the output quadrature, carrying information about the qubit state and measured by a homodyne setup with a detection angle ϕ_h , is given by

$$\hat{\mathcal{Z}}_{\text{out}}(t) = \hat{a}_{s,\text{out}}(t)e^{-i\phi_h} + \hat{a}_{s,\text{out}}^\dagger(t)e^{i\phi_h}. \quad (\text{S37})$$

To evaluate the SNR, which is an essential parameter quantifying the homodyne detection, we define the following measurement operator,

$$\hat{M} = \sqrt{\kappa_s} \int_0^\tau dt \hat{\mathcal{Z}}_{\text{out}}(t), \quad (\text{S38})$$

where τ is the measurement time. Its average, $\langle \hat{M} \rangle$, is the qubit-state-dependent measurement signal, while the variance of the noise operator $\hat{M}_N = \hat{M} - \langle \hat{M} \rangle$ represents the measurement noise. Then, the SNR reads

$$\text{SNR} = \frac{|\langle \hat{M} \rangle_\uparrow - \langle \hat{M} \rangle_\downarrow|}{\sqrt{\langle \hat{M}_N^2 \rangle_\uparrow + \langle \hat{M}_N^2 \rangle_\downarrow}}, \quad (\text{S39})$$

where the arrows \uparrow and \downarrow refers to the excited and ground states of the qubit.

Note that the longitudinal coupling in fact offers a qubit-state-dependent resonant driving for the signal mode \hat{a}_s , and can act as an internal measurement tone. In this case, the input measurement tone is no longer needed, such that the average of the input operator $\hat{a}_{s,\text{in}}(t)$ equals zero, i.e., $\langle \hat{a}_{s,\text{in}}(t) \rangle = 0$, and then the correlations for $\hat{a}_{s,\text{in}}(t)$ are given by

$$\langle \hat{a}_{s,\text{in}}(t) \hat{a}_{s,\text{in}}^\dagger(t') \rangle = \delta(t-t'), \quad (\text{S40})$$

$$\langle \hat{a}_{s,\text{in}}^\dagger(t) \hat{a}_{s,\text{in}}(t') \rangle = \langle \hat{a}_{s,\text{in}}(t) \hat{a}_{s,\text{in}}(t') \rangle = 0. \quad (\text{S41})$$

Under the initial condition $\langle \hat{a}_s(0) \rangle = 0$, we find

$$\begin{aligned}\langle \hat{M} \rangle_\uparrow - \langle \hat{M} \rangle_\downarrow = & \frac{8\chi_z\kappa_s}{(\kappa_s^2 - 16\Omega_{2\text{pd}}^2)^2} \left\{ [\kappa_s^2(2 - \kappa_s\tau) + 16(2 + \kappa_s\tau)\Omega_{2\text{pd}}^2] \sin(\phi_h - \phi_z) \right. \\ & \left. - 4\Omega_{2\text{pd}} [\kappa_s(4 - \kappa_s\tau) + 16\Omega_{2\text{pd}}^2\tau] \cos(\phi_h + \phi_z - 2\phi_{2\text{pd}}) \right\} \\ & + \mathcal{F}_- e^{-\frac{1}{2}(\kappa_s - 4\Omega_{2\text{pd}})\tau} + \mathcal{F}_+ e^{-\frac{1}{2}(\kappa_s + 4\Omega_{2\text{pd}})\tau},\end{aligned}\quad (\text{S42})$$

with

$$\mathcal{F}_\pm = \frac{8\chi_z\kappa_s}{(\kappa_s \pm 4\Omega_{2\text{pd}})^2} [\cos(\phi_h + \phi_z - 2\phi_{2\text{pd}}) \pm \sin(\phi_h - \phi_z)]. \quad (\text{S43})$$

Here, we have assumed $t_0 = 0$ for simplicity.

Furthermore, the quantum fluctuation of the output field $\hat{a}_{s,\text{out}}(t)$, given by $\hat{f}_{\text{out}}(t) = \hat{a}_{s,\text{out}}(t) - \langle \hat{a}_{s,\text{out}}(t) \rangle$, is found to be

$$\begin{aligned} \hat{f}_{\text{out}}(t) = & \hat{a}_{s,\text{in}}(t) - \kappa_s \int_{-\infty}^t ds \cosh[2\Omega_{2\text{pd}}(t-s)] e^{-\kappa_s(t-s)/2} \hat{a}_{s,\text{in}}(s) \\ & + ie^{i2\phi_{2\text{pd}}} \kappa_s \int_{-\infty}^t ds \sinh[2\Omega_{2\text{pd}}(t-s)] e^{-\kappa_s(t-s)/2} \hat{a}_{s,\text{in}}^\dagger(s). \end{aligned} \quad (\text{S44})$$

Here, we have assumed that before the measurement starts (i.e., the longitudinal qubit-field coupling starts), the system (i.e., the semiclassical DPA) is already in the steady state. Thus in Eq. (S44), the lower limit of integration has been extended to $-\infty$. The measurement noise, when expressed in terms of $\hat{f}_{\text{out}}(t)$, is

$$\begin{aligned} \langle \hat{M}_N^2 \rangle = & \kappa_s \int_0^\tau \int_0^\tau dt_1 dt_2 \left[\langle \hat{f}_{\text{out}}^\dagger(t_1) \hat{f}_{\text{out}}(t_2) \rangle + \langle \hat{f}_{\text{out}}(t_1) \hat{f}_{\text{out}}^\dagger(t_2) \rangle \right. \\ & \left. + \langle \hat{f}_{\text{out}}(t_1) \hat{f}_{\text{out}}(t_2) \rangle e^{-i2\phi_h} + \langle \hat{f}_{\text{out}}^\dagger(t_1) \hat{f}_{\text{out}}^\dagger(t_2) \rangle e^{i2\phi_h} \right], \end{aligned} \quad (\text{S45})$$

and after a straightforward but tedious calculation is found as follows:

$$\begin{aligned} \langle \hat{M}_N^2 \rangle = & \kappa_s \tau + \frac{16\kappa_s^2 \Omega_{2\text{pd}}}{(\kappa_s^2 - 16\Omega_{2\text{pd}}^2)^3} \left\{ [\kappa_s^3(2 - \kappa_s \tau) + 32(3\kappa_s + 8\Omega_{2\text{pd}}^2 \tau) \Omega_{2\text{pd}}^2] \sin[2(\phi_h - \phi_{2\text{pd}})] \right. \\ & \left. - 8\kappa_s^2(3 - \kappa_s \tau) \Omega_{2\text{pd}} - 128(1 + \kappa_s \tau) \Omega_{2\text{pd}}^3 \right\} \\ & + \mathcal{Z}_- e^{-\frac{1}{2}(\kappa_s - 4\Omega_{2\text{pd}})\tau} - \mathcal{Z}_+ e^{-\frac{1}{2}(\kappa_s + 4\Omega_{2\text{pd}})\tau}, \end{aligned} \quad (\text{S46})$$

where

$$\mathcal{Z}_\pm = \frac{16\kappa_s^2 \Omega_{2\text{pd}}}{(\kappa_s \pm 4\Omega_{2\text{pd}})^3} \{1 \pm \sin[2(\phi_h - \phi_{2\text{pd}})]\}. \quad (\text{S47})$$

From Eq. (S46) the noise is minimized by choosing $\phi_h - \phi_{2\text{pd}} = \pi/4$, corresponding to the homodyne detection along the direction of squeezing. Then according to Eq. (S42), the signal separation $|\langle \hat{M} \rangle_\uparrow - \langle \hat{M} \rangle_\downarrow|$ is maximized for $\phi_h - \phi_z = \pi/2$.

For these optimal phases, below we discuss the SNR. Let us first consider a special case of $\Omega_{2\text{pd}} = 0$, corresponding to the standard longitudinal readout with no squeezing. In such a case, the SNR is given by [S11]

$$\text{SNR}_z^{\text{std}} = \frac{6}{\kappa_s \tau} \text{SNR}_x^{\text{std}} = \chi_z \tau \sqrt{2\kappa_s \tau}, \quad (\text{S48})$$

for a short-time measurement (i.e., $\kappa_s \tau \ll 1$). Here, $\text{SNR}_x^{\text{std}} = \varepsilon (\kappa_s \tau)^{5/2} / (3\sqrt{2}\kappa_s)$ refers to the short-time SNR of the standard dispersive readout with a measurement tone of amplitude ε [S12]. For comparison, we have assumed the amplitude ε to be equal to the longitudinal coupling strength χ_z . Clearly, the longitudinal readout requires much shorter measurement times, compared to the dispersive readout.

We now consider the SNR for any $\Omega_{2\text{pd}}$ that can keep the system stable, i.e., $\Omega_{2\text{pd}} < \kappa_s/2$. For the short-time measurement, i.e., $\kappa_s \tau \ll 1$ or $(\kappa_s \pm 4\Omega_{2\text{pd}}) \ll 1$, the signal separation is found to be

$$|\langle \hat{M} \rangle_\uparrow - \langle \hat{M} \rangle_\downarrow| \simeq 2\chi_z \kappa_s \tau^2, \quad (\text{S49})$$

up to second order, and likewise, the measurement noise is reduced to

$$\langle \hat{M}_N^2 \rangle \simeq \kappa_s \tau - \frac{4\Omega_{2\text{pd}}}{\kappa_s + 4\Omega_{2\text{pd}}} (\kappa_s \tau)^2 \simeq \kappa_s \tau. \quad (\text{S50})$$

We find that both the short-time signal and noise are almost unaffected by the twp-photon driving $\Omega_{2\text{pd}}$ or equivalently by intracavity squeezing. In turn, the optimal SNR is found to be

$$\text{SNR}_z^{\text{sc}} \simeq \text{SNR}_z^{\text{std}}. \quad (\text{S51})$$

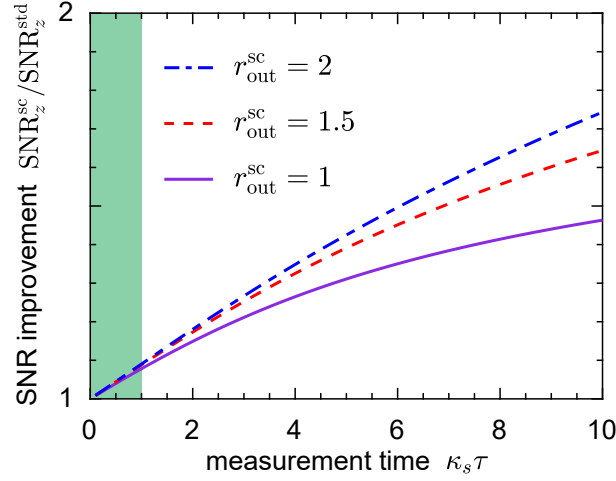


FIG. S3. SNR improvement, i.e., $\text{SNR}_z^{\text{sc}}/\text{SNR}_z^{\text{std}}$, of longitudinal qubit readout using intracavity squeezing of the semiclassical degenerate parametric amplifier for $r_{\text{out}}^{\text{sc}} = 1, 1.5$, and 2 . The SNR is calculated using Eqs. (S42) and (S46) for $\phi_h = \phi_{2\text{pd}} + \pi/4 = \phi_z + \pi/2$. The green shaded area refers to the regime of most interest in experiments.

This implies that the semiclassical-DPA intracavity squeezing does not improve the SNR for the short-time measurement. In Fig. S3, we plot the SNR improvement, i.e., the ratio $\text{SNR}_z^{\text{sc}}/\text{SNR}_z^{\text{std}}$, as a function of the measurement time $\kappa_s \tau$. In this figure, we define the parameter

$$r_{\text{out}}^{\text{sc}} = \ln \left(\frac{\kappa_s + 4\Omega_{2\text{pd}}}{\kappa_s - 4\Omega_{2\text{pd}}} \right), \quad (\text{S52})$$

which characterizes the degree of squeezing of the output field of the semiclassical DPA in the absence of the qubit. It can be seen that the SNR is almost unaffected in the regime $\tau \leq 1/\kappa_s$, which is of most interest in experiments.

Moreover, for the long-time measurement, i.e., $\kappa_s \tau \gg 1$ or $(\kappa_s \pm 4\Omega_{2\text{pd}}) \gg 1$, an exponential improvement in the SNR can be obtained as

$$\text{SNR}_z^{\text{sc}} \simeq \frac{\kappa_s}{\kappa_s + 4\Omega_{2\text{pd}}} \exp(r_{\text{out}}^{\text{sc}}) \text{SNR}_z^{\text{std}}. \quad (\text{S53})$$

For example, choosing $r_{\text{out}}^{\text{sc}} = 2$ ($\simeq 17$ dB) can give a more than four-fold improvement in the long-time limit. However, as shown in Fig. S3, even with a long measurement time of up to $\tau = 10/\kappa_s$, the output-field squeezing of $r_{\text{out}}^{\text{sc}} = 2$ can only lead to a modest improvement of the SNR by a factor of $\simeq 1.7$. This means that in order to obtain the exponential improvement given in Eq. (S53), the measurement time needs to be extremely long, which is infeasible in experiments. Hence, the semiclassical-DPA intracavity squeezing *cannot* significantly improve the SNR during a practically feasible measurement time, even with a strong output-field squeezing.

To understand this result of no significant improvement of practical interest in experiments, we now turn to phase space. In order to describe the Wigner function of the output field, we define the temporal mode [S13, S14]

$$\hat{A} = \frac{1}{\sqrt{\tau}} \int_0^\tau dt \hat{a}_{s,\text{out}}(t). \quad (\text{S54})$$

The resulting bosonic commutation relation $[\hat{A}, \hat{A}^\dagger] = 1$ allows us to introduce two conjugate quadratures,

$$\hat{X}_{\text{out}} = \frac{1}{2} (\hat{A} + \hat{A}^\dagger), \quad \text{and} \quad \hat{Y}_{\text{out}} = \frac{1}{2i} (\hat{A} - \hat{A}^\dagger), \quad (\text{S55})$$

which satisfy $[\hat{X}_{\text{out}}, \hat{Y}_{\text{out}}] = i$. With these quadratures, the Wigner function of the output field can be calculated as

$$W(X_{\text{out}}, Y_{\text{out}}) = \frac{1}{2\pi \sqrt{\text{Det}(\mathbf{D})}} \exp \left(-\frac{1}{2} \mathbf{G}^T \mathbf{D}^{-1} \mathbf{G} \right), \quad (\text{S56})$$

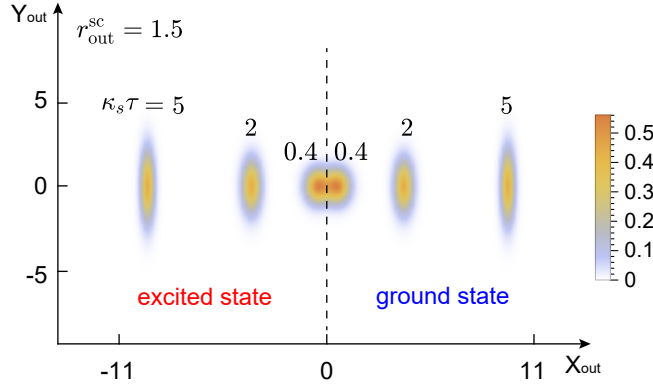


FIG. S4. Phase-space representation of longitudinal qubit readout using intracavity squeezing of the semiclassical degenerate parametric amplifier. We chose, for $r_{\text{out}}^{\text{sc}} = 1.5$ ($\simeq 13$ dB), three different measurement times: $\kappa_s \tau = 0.4, 2$, and 5 . The resulting Wigner functions on the left and right of the vertical dashed line correspond to the excited and ground states of the qubit, respectively. The degree of squeezing of the measurement noise strongly depends on the measurement time.

where

$$\mathbf{G} = \left(X_{\text{out}} - \langle \hat{X}_{\text{out}} \rangle, Y_{\text{out}} - \langle \hat{Y}_{\text{out}} \rangle \right)^T, \quad (\text{S57})$$

$$\mathbf{D} = \begin{pmatrix} \langle \hat{X}_{\text{out}}^2 \rangle - \langle \hat{X}_{\text{out}} \rangle^2 & \langle \hat{X}_{\text{out}} \hat{Y}_{\text{out}} + \hat{Y}_{\text{out}} \hat{X}_{\text{out}} \rangle / 2 - \langle \hat{X}_{\text{out}} \rangle \langle \hat{Y}_{\text{out}} \rangle \\ \langle \hat{X}_{\text{out}} \hat{Y}_{\text{out}} + \hat{Y}_{\text{out}} \hat{X}_{\text{out}} \rangle / 2 - \langle \hat{X}_{\text{out}} \rangle \langle \hat{Y}_{\text{out}} \rangle & \langle \hat{Y}_{\text{out}}^2 \rangle - \langle \hat{Y}_{\text{out}} \rangle^2 \end{pmatrix}. \quad (\text{S58})$$

We show in Fig. S4 the Wigner functions in phase space for different measurement times and for the ground and excited states of the qubit. The degree of squeezing of the measurement noise increases from the initial value zero as the measurement time increases, and then tends asymptotically towards the limit value r_{out} . The practically unsqueezed measurement noise in the regime $\kappa_s \tau \leq 1$ is the physical reason for almost no improvement in the SNR for the short-time measurement.

S6. Improved longitudinal qubit readout using our fully-quantum-DPA intracavity squeezing

Following the same method as in Sec. , we here derive and analyze the measurement signal, measurement noise, and SNR for the longitudinal readout of a qubit embedded in the fully quantum DPA. In our approach, the qubit is coupled to the pump mode, rather than to the signal mode as described in Sec. . We demonstrate that, compared to the case of using the semiclassical-DPA intracavity squeezing, *the predicted fully-quantum-DPA intracavity squeezing enables an exponential improvement in the SNR for any measurement time, thus yielding a faster and higher-SNR (i.e., higher-fidelity) qubit readout.*

With the Hamiltonian \hat{H}_z^{fq} in Eq. (12) in the main article, the quantum Langevin equations of motion for the modes \hat{a}_p and $\hat{\beta}_s$ are

$$\dot{\hat{a}}_p = -i\sigma\chi_z e^{i\phi_z} - i \left(G_- \hat{\beta}_s + G_+ \hat{\beta}_s^\dagger \right) - \frac{\kappa_p}{2} \hat{a}_p - \sqrt{\kappa_p} \hat{a}_{p,\text{in}}(t), \quad (\text{S59})$$

$$\dot{\hat{\beta}}_s = -i \left(G_- \hat{a}_p + G_+ \hat{a}_p^\dagger \right) - \frac{\kappa_s}{2} \hat{\beta}_s - \sqrt{\kappa_s} \hat{\beta}_{s,\text{in}}. \quad (\text{S60})$$

As was assumed for the generation of the strong steady-state intracavity squeezing, the photon loss rate κ_s of the mode $\hat{\beta}_s$ is sufficiently large, such that we can set $\dot{\hat{\beta}}_s = 0$ to adiabatically eliminate the mode $\hat{\beta}_s$. This leads to the following adiabatic equation of motion for the mode \hat{a}_p ,

$$\dot{\hat{a}}_p = -i\sigma\chi_z e^{i\phi_z} - \frac{\kappa}{2} \hat{a}_p - \sqrt{\kappa} \hat{\mathcal{A}}_{\text{in}}(t). \quad (\text{S61})$$

Here, the noise operator $\hat{\mathcal{A}}_{\text{in}}(t) = \frac{1}{\sqrt{\kappa}} \left[\sqrt{\kappa_p^{\text{ad}}} \hat{a}_{p,\text{in}}^{\text{ad}}(t) + \sqrt{\kappa_p} \hat{a}_{p,\text{in}}(t) \right]$ describes the overall input noise. The pump mode

\hat{a}_p is then found, after formally integrating, to be

$$\begin{aligned} \hat{a}_p(t) &= e^{-\kappa(t-t_0)/2} \hat{a}_p(t_0) \\ &\quad - i \frac{2}{\kappa} \sigma \chi_z e^{i\phi_z} \left[1 - e^{-\kappa(t-t_0)/2} \right] - \sqrt{\kappa} \int_{t_0}^t e^{-\kappa(t-s)/2} \hat{\mathcal{A}}_{\text{in}}(s) ds. \end{aligned} \quad (\text{S62})$$

As mentioned in Sec. , the longitudinal coupling can be thought of as an internal measurement tone, and there is no input or external measurement tone. In this case, $\langle \hat{\beta}_{s,\text{in}}(t) \rangle = \langle \hat{\mathcal{A}}_{\text{in}}(t) \rangle = 0$. Moreover, the correlations for $\hat{\beta}_{s,\text{in}}(t)$, which approximately describe the vacuum noise of the mode $\hat{\beta}_s$, are

$$\langle \hat{\beta}_{s,\text{in}}(t) \hat{\beta}_{s,\text{in}}^\dagger(t') \rangle = \delta(t - t'), \quad (\text{S63})$$

$$\langle \hat{\beta}_{s,\text{in}}^\dagger(t) \hat{\beta}_{s,\text{in}}(t') \rangle = \langle \hat{\beta}_{s,\text{in}}(t) \hat{\beta}_{s,\text{in}}(t') \rangle = 0, \quad (\text{S64})$$

and, as a consequence, the correlations for $\hat{\mathcal{A}}_{\text{in}}(t)$ are

$$\langle \hat{\mathcal{A}}_{\text{in}}(t) \hat{\mathcal{A}}_{\text{in}}^\dagger(t') \rangle = \left[\frac{1}{4\mathcal{C} + 1} + \frac{4\mathcal{C}}{4\mathcal{C} + 1} \cosh^2(r_p) \right] \delta(t - t'), \quad (\text{S65})$$

$$\langle \hat{\mathcal{A}}_{\text{in}}^\dagger(t) \hat{\mathcal{A}}_{\text{in}}(t') \rangle = \frac{4\mathcal{C}}{4\mathcal{C} + 1} \sinh^2(r_p) \delta(t - t'), \quad (\text{S66})$$

$$\langle \hat{\mathcal{A}}_{\text{in}}(t) \hat{\mathcal{A}}_{\text{in}}(t') \rangle = - \frac{2\mathcal{C}}{4\mathcal{C} + 1} \sinh(2r_p) \delta(t - t'). \quad (\text{S67})$$

Here, $\mathcal{C} = \mathcal{G}^2/(\kappa_s \kappa_p)$ is the cooperativity of the DPA. It is seen that the correlation in Eq. (S65) includes two contributions, one from the natural photon loss of the pump mode \hat{a}_p and the other from the adiabatic effect of the signal Bogoliubov mode $\hat{\beta}_s$.

It follows, according to the input-output relation $\hat{\mathcal{A}}_{\text{out}}(t) = \hat{\mathcal{A}}_{\text{in}}(t) + \sqrt{\kappa} \hat{a}_p(t)$, that the signal separation is found to be

$$\left| \langle \hat{M} \rangle_\uparrow - \langle \hat{M} \rangle_\downarrow \right| = 8\chi_z \tau |\sin(\phi_h - \phi_z)| \left\{ 1 - \frac{2}{\kappa\tau} [1 - \exp(-\kappa\tau/2)] \right\}. \quad (\text{S68})$$

Here, we have assumed $t_0 = 0$ as usual. This signal separation is the same as obtained in the standard longitudinal readout with no squeezing [S11, S15]. Moreover, the quantum fluctuation noise of the output field now is $\hat{f}_{\text{out}}(t) = \hat{\mathcal{A}}_{\text{out}}(t) - \langle \hat{\mathcal{A}}_{\text{out}}(t) \rangle$, and evolves as

$$\hat{f}_{\text{out}}(t) = \hat{\mathcal{A}}_{\text{in}}(t) - \kappa \int_{-\infty}^t \exp[-\kappa(t-s)/2] \hat{\mathcal{A}}_{\text{in}}(s) ds. \quad (\text{S69})$$

Here, the lower limit of integration has been extended to $-\infty$ for the same reason as mentioned in Sec. . The expression of the measurement noise is the same as in Eq. (S45) but now replacing $\kappa_s \mapsto \kappa$, and, then, a straightforward calculation leads to

$$\langle \hat{M}_N^2 \rangle = \kappa\tau \left\{ \frac{1}{4\mathcal{C} + 1} + \frac{4\mathcal{C}}{4\mathcal{C} + 1} [\cosh(2r_p) - \cos(2\phi_h) \sinh(2r_p)] \right\}. \quad (\text{S70})$$

As long as $\mathcal{C} \gg e^{2r_p}/4$, then $\langle \hat{M}_N^2 \rangle$ is reduced to the measurement noise of the longitudinal readout with injecting a squeezed reservoir in the ideal case of no transmission and injection losses [S11], i.e.,

$$\langle \hat{M}_N^2 \rangle_{\text{ideal}} = \kappa\tau [\cosh(2r_p) - \cos(2\phi_h) \sinh(2r_p)]. \quad (\text{S71})$$

By choosing $\phi_z = \pi/2$ and $\phi_h = 0$, the optimal SNR of the longitudinal readout using the fully-quantum-DPA intracavity squeezing is given by

$$\text{SNR}_z^{\text{fq}} = \sqrt{\frac{4\mathcal{C} + 1}{4\mathcal{C} \exp(-2r_p) + 1}} \text{SNR}_z^{\text{std}}, \quad (\text{S72})$$

which shows a significant improvement in the SNR. In particular, an exponential improvement,

$$\text{SNR}_z^{\text{fq}} \simeq \exp(r_p) \text{SNR}_z^{\text{std}}, \quad (\text{S73})$$

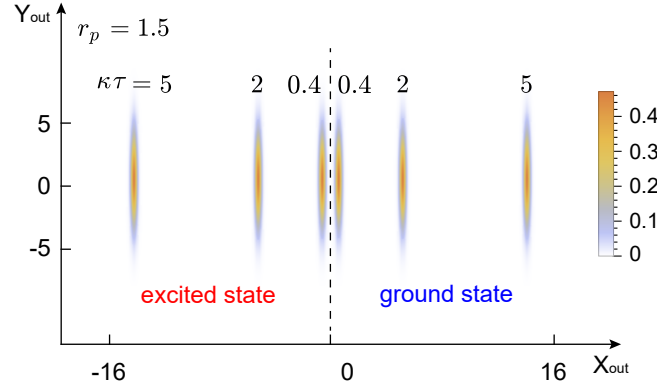


FIG. S5. Phase-space representation of longitudinal qubit readout using intracavity squeezing of the fully quantum degenerate parametric amplifier. We chose, for $r_{\text{out}} = 1.5$ ($\simeq 13$ dB), three different measurement times: $\kappa\tau = 0.4, 2$, and 5 . The resulting Wigner functions on the left and right of the vertical dashed line correspond to the excited and ground states of the qubit, respectively. The strong squeezing of the measurement noise is independent of the measurement time.

can be achieved for $\mathcal{C} \gg e^{2r_p}/4$. We note that Eqs. (S72) and (S73) hold for *any* measurement time. This is because the degree of squeezing of the measurement noise, i.e., $\langle \hat{M}_N^2 \rangle / \kappa\tau$, is independent of the measurement time τ [see Eq. (S70)], and particularly is equal to the degree of intracavity squeezing for $\phi_h = 0$, i.e., $\langle \hat{M}_N^2 \rangle / \kappa\tau = (\xi_p^2)_{\text{ss}} = [1 + 4\mathcal{C} \exp(-2r_p)] / (1 + 4\mathcal{C})$. This becomes more apparent in phase space shown in Fig. S5. We find that a short measurement time of $\tau = 0.4/\kappa$ can well resolve the measurement signals associated with the ground and excited states of the qubit. This is in stark contrast to what we have already shown in Fig. S4, where the same measurement time (i.e., $\tau = 0.4/\kappa_s$) leads to a high degree of overlap of the measurement signals, such that they cannot be resolved. In order to compare, we here have assumed κ_s in Fig. S4 and κ in Fig. S5 to be equal. Thus, our approach can enable a faster and higher-SNR qubit readout.

S7. Possible implementations of our approach for improving longitudinal qubit readout

The longitudinal qubit-field coupling can be directly realized via circuit design in circuit quantum electrodynamics [S16–S22]. Alternatively, some synthetic approaches, e.g., strongly driving the qubit-field dispersive coupling, have also been proposed and even demonstrated in experiments [S15, S23–S27]. In this section, as an example, we discuss in detail a possible implementation of the Hamiltonian \hat{H}_z^{fq} in Eq. (12) in a synthetic manner. In particular, we refer to the experimental implementation reported in Ref. [S26], where the longitudinal coupling is synthesized with driving the qubit at the cavity frequency.

Let us now assume that the qubit is driven with phase ϕ_z , amplitude \mathcal{E}_q^{d} , and frequency ω_q^{d} . The total Hamiltonian accordingly is given, in the frame rotating at ω_d , by

$$\begin{aligned} \hat{H}_T = \hat{H} + \frac{1}{2}\Delta_q \hat{\sigma}_z + g_q (\hat{\sigma}_- \hat{a}_p^\dagger + \text{H.c.}) \\ + \mathcal{E}_q^{\text{d}} \left[e^{i\phi_z} \hat{\sigma}_- e^{-i(\omega_d - \omega_q^{\text{d}})t} + \text{H.c.} \right], \end{aligned} \quad (\text{S74})$$

where \hat{H} has been given in the main article, $\hat{\sigma}_\pm$ are the raising/lowering operators of the qubit, g_q is the strength of the coupling of the qubit to the pump mode, and $\Delta_q = \omega_q - \omega_d$ is the detuning of the qubit from the driving of the pump mode. We follow the same steps listed in Sec. to find that the dynamics of the total system can be described by the following Hamiltonian

$$\begin{aligned} \hat{H}'_T = \hat{H}_{\text{eff}} + g_q \left(\hat{\sigma}_- \hat{a}_p^\dagger e^{-i\Delta_q^{\text{d}}t} + \text{H.c.} \right) \\ + \mathcal{E}_q^{\text{d}} \left(\hat{\sigma}_- e^{i\phi_z} e^{-i\Delta_q^{\text{d}}t} + \text{H.c.} \right) \\ + g_q \alpha_p^{\text{d}} \left(\hat{\sigma}_- e^{-i\Delta_q^{\text{d}}t} + \text{H.c.} \right). \end{aligned} \quad (\text{S75})$$

Here, \hat{H}_{eff} is already given in Eq. (7) in the main article, and we have assumed that $\omega_q - \omega_p = \omega_q - \omega_q^{\text{d}} = \Delta_q^{\text{d}}$. Note

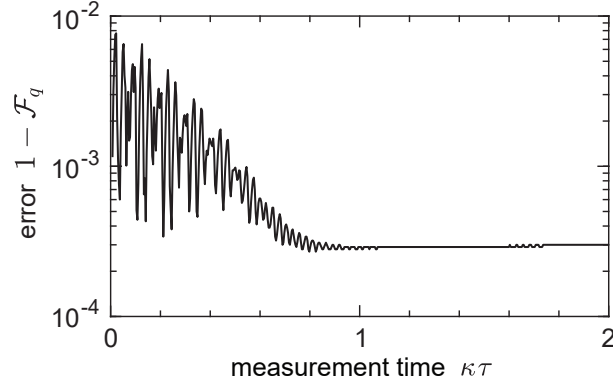


FIG. S6. State error, $1 - \mathcal{F}_q$, as a function of the measurement time $\kappa\tau$. We assumed that $g_q = q$, $\mathcal{E}_q^d = 10g_q$, $\phi_z = \pi/2$, $\Delta_q^d = 200g_q$, $\Delta_q = \Delta_q^d + \Delta_p$, $G_+ = 0.7G_-$, and other parameters associated with \hat{H}_{eff} are the same as those in Fig. 1(b). We assumed that the qubit is initially in the state $(|g\rangle + |e\rangle)/\sqrt{2}$, while the signal and pump modes are in the steady state given by \hat{H}_{eff} .

that the detuned drivings of the qubit, which are associated with the field amplitudes α_p^\pm induced by the ω_\pm drivings of the signal mode, have been neglected since $\alpha_p^\pm \ll \alpha_p^d$.

We further assume $\Delta_q^d \gg \{g_q, \mathcal{E}_q^d\}$ and $\Delta_q \gg g_q\alpha_p^d$, justifying for a perturbative treatment of the second, third and fourth terms of \hat{H}'_T using the formalism of Ref. [S1]. We then find that

$$\hat{H}'_T \approx \hat{H}_{\text{eff}} + \chi_z \hat{\sigma}_z (\hat{a}_p e^{-i\phi_z} + \hat{a}_p^\dagger e^{i\phi_z}) + \chi_x \hat{a}_p^\dagger \hat{a}_p \hat{\sigma}_z, \quad (\text{S76})$$

where

$$\chi_z = \mathcal{E}_q^d g_q / \Delta_q^d, \quad \text{and} \quad \chi_x = g_q^2 / \Delta_q^d \quad (\text{S77})$$

are the strengths of the longitudinal and dispersive couplings between the qubit and the pump mode, respectively. In Eq. (S76), we have subtracted the term describing the resonance shift of the qubit, i.e., $\frac{1}{2}\delta_z \hat{\sigma}_z$, where

$$\delta_z = [g_q^2 + 2(\mathcal{E}_q^d)^2] / \Delta_q^d + 2(g_q\alpha_p^d)^2 / \Delta_q. \quad (\text{S78})$$

This is because this term can be completely eliminated in a proper frame. Under the assumption of $\mathcal{E}_p^d \gg g_q$, the longitudinal coupling χ_z is much stronger than the dispersive coupling χ_x , so that the latter can be neglected, yielding

$$\hat{H}'_T \simeq \hat{H}_{\text{eff}} + \chi_z \hat{\sigma}_z (\hat{a}_p e^{-i\phi_z} + \hat{a}_p^\dagger e^{i\phi_z}). \quad (\text{S79})$$

This is the Hamiltonian \hat{H}_z^{fq} in Eq. (12) in the main article.

To confirm the validity of Eq. (S79), we perform numerical simulations, as shown in Fig. S6. Specifically, we calculate the fidelity, \mathcal{F}_q , of two qubit states that are given by the evolution under the two Hamiltonians in Eqs. (S75) and (S79), respectively, from the same initial state. In Fig. S6, we assume that the initial state of the qubit is $(|g\rangle + |e\rangle)/\sqrt{2}$. At the same time, the initial state of the signal and pump modes is assumed to be the steady state given by \hat{H}_{eff} , indicating that when the measurement starts, a steady-state squeezing has already been generated. It can be seen in Fig. S6 that during a long measurement time, the state error, $1 - \mathcal{F}_q$, can be kept well below 10^{-2} for some modest parameters.

-
- [S1] O. Gamel and D. F. V. James, “Time-averaged quantum dynamics and the validity of the effective Hamiltonian model,” *Phys. Rev. A* **82**, 052106 (2010).
- [S2] Z. Leghtas *et al.*, “Confining the state of light to a quantum manifold by engineered two-photon loss,” *Science* **347**, 853 (2015).
- [S3] S. Touzard *et al.*, “Coherent Oscillations inside a Quantum Manifold Stabilized by Dissipation,” *Phys. Rev. X* **8**, 021005 (2018).
- [S4] R. Lescanne, M. Villiers, T. Peronnin, A. Sarlette, M. Delbecq, B. Huard, T. Kontos, M. Mirrahimi, and Z. Leghtas, “Exponential suppression of bit-flips in a qubit encoded in an oscillator,” *Nat. Phys.* **16**, 509 (2020).
- [S5] C. W. S. Chang, C. Sabín, P. Forn-Díaz, F. Quijandría, A. M. Vadiraj, I. Nsanzineza, G. Johansson, and C. M. Wilson, “Observation of three-photon spontaneous parametric down-conversion in a superconducting parametric cavity,” *Phys. Rev. X* **10**, 011011 (2020).
- [S6] A. Vrajitoarea, Z. Huang, P. Groszkowski, J. Koch, and A. A Houck, “Quantum control of an oscillator using a stimulated Josephson nonlinearity,” *Nat. Phys.* **16**, 211 (2020).
- [S7] X. Guo, C.-L. Zou, and H. X. Tang, “Second-harmonic generation in aluminum nitride microrings with 2500%/W conversion efficiency,” *Optica* **3**, 1126–1131 (2016).
- [S8] A. W. Bruch, X. Liu, J. B. Surya, C.-L. Zou, and H. X. Tang, “On-chip $\chi^{(2)}$ microring optical parametric oscillator,” *Optica* **6**, 1361–1366 (2019).
- [S9] J.-Q. Wang, Y.-H. Yang, M. Li, X.-X. Hu, J. B. Surya, X.-B. Xu, C.-H. Dong, G.-C. Guo, H. X. Tang, and C.-L. Zou, “Efficient Frequency Conversion in a Degenerate $\chi^{(2)}$ Microresonator,” *Phys. Rev. Lett.* **126**, 133601 (2021).
- [S10] C. W. Gardiner and M. J. Collett, “Input and output in damped quantum systems: Quantum stochastic differential equations and the master equation,” *Phys. Rev. A* **31**, 3761–3774 (1985).
- [S11] N. Didier, J. Bourassa, and A. Blais, “Fast Quantum Nondemolition Readout by Parametric Modulation of Longitudinal Qubit-Oscillator Interaction,” *Phys. Rev. Lett.* **115**, 203601 (2015).
- [S12] X. Wang, A. Miranowicz, and F. Nori, “Ideal Quantum Nondemolition Readout of a Flux Qubit without Purcell Limitations,” *Phys. Rev. Applied* **12**, 064037 (2019).
- [S13] I. Strandberg, G. Johansson, and F. Quijandría, “Wigner negativity in the steady-state output of a kerr parametric oscillator,” *Phys. Rev. Research* **3**, 023041 (2021).
- [S14] Y. Lu, I. Strandberg, F. Quijandría, G. Johansson, S. Gasparinetti, and P. Delsing, “Propagating Wigner-Negative States Generated from the Steady-State Emission of a Superconducting Qubit,” *Phys. Rev. Lett.* **126**, 253602 (2021).
- [S15] S. Touzard, A. Kou, N. E. Frattini, V. V. Sivak, S. Puri, A. Grimm, L. Frunzio, S. Shankar, and M. H. Devoret, “Gated Conditional Displacement Readout of Superconducting Qubits,” *Phys. Rev. Lett.* **122**, 080502 (2019).
- [S16] Y.-x. Liu *et al.*, “Controllable Coupling between Flux Qubits,” *Phys. Rev. Lett.* **96**, 067003 (2006).
- [S17] A. J. Kerman, “Quantum information processing using quasiclassical electromagnetic interactions between qubits and electrical resonators,” *New J. Phys.* **15**, 123011 (2013).
- [S18] P.-M. Billangeon, J. S. Tsai, and Y. Nakamura, “Circuit-QED-based scalable architectures for quantum information processing with superconducting qubits,” *Phys. Rev. B* **91**, 094517 (2015).
- [S19] P.-M. Billangeon, J. S. Tsai, and Y. Nakamura, “Scalable architecture for quantum information processing with superconducting flux qubits based on purely longitudinal interactions,” *Phys. Rev. B* **92**, 020509(R) (2015).
- [S20] S. Richer and D. DiVincenzo, “Circuit design implementing longitudinal coupling: A scalable scheme for superconducting qubits,” *Phys. Rev. B* **93**, 134501 (2016).
- [S21] S. Richer, N. Maleeva, S. T. Skacel, I. M. Pop, and D. DiVincenzo, “Inductively shunted transmon qubit with tunable transverse and longitudinal coupling,” *Phys. Rev. B* **96**, 174520 (2017).
- [S22] R. Stassi and F. Nori, “Long-lasting quantum memories: Extending the coherence time of superconducting artificial atoms in the ultrastrong-coupling regime,” *Phys. Rev. A* **97**, 033823 (2018).
- [S23] J. Q. You and F. Nori, “Quantum information processing with superconducting qubits in a microwave field,” *Phys. Rev. B* **68**, 064509 (2003).
- [S24] A. Blais, J. Gambetta, A. Wallraff, D. I. Schuster, S. M. Girvin, M. H. Devoret, and R. J. Schoelkopf, “Quantum-information processing with circuit quantum electrodynamics,” *Phys. Rev. A* **75**, 032329 (2007).
- [S25] A. Eddins, S. Schreppler, D. M. Toyli, L. S. Martin, S. Hacoen-Gourgy, L. C. G. Govia, H. Ribeiro, A. A. Clerk, and I. Siddiqi, “Stroboscopic Qubit Measurement with Squeezed Illumination,” *Phys. Rev. Lett.* **120**, 040505 (2018).
- [S26] J. Ikonen, J. Goetz, J. Ilves, A. Keränen, A. M. Gunyho, M. Partanen, K. Y. Tan, D. Hazra, L. Grönberg, V. Vesterinen, S. Simbierowicz, J. Hassel, and M. Möttönen, “Qubit Measurement by Multichannel Driving,” *Phys. Rev. Lett.* **122**, 080503 (2019).
- [S27] R. Dassonneville *et al.*, “Fast High-Fidelity Quantum Nondemolition Qubit Readout via a Nonperturbative Cross-Kerr Coupling,” *Phys. Rev. X* **10**, 011045 (2020).